

## Modification of Binuclear Pt–Tl Bonded Complexes by Attaching Bipyridine Ligands to the Thallium Site

Guibin Ma,<sup>‡</sup> Mikael Kritikos,<sup>†</sup> Mikhail Maliarik,<sup>§</sup> and Julius Glaser<sup>\*</sup>

Department of Chemistry, Royal Institute of Technology (KTH), S-100 44 Stockholm, Sweden

Received May 27, 2003

Complex formation of monomeric thallium(III) species with 2,2'-bipyridine (bipy) in dimethyl sulfoxide (dmsO) and acetonitrile solutions was studied by means of multinuclear (<sup>1</sup>H, <sup>13</sup>C, and <sup>205</sup>Tl) NMR spectroscopy. For the first time, NMR signals of the individual species [Tl(bipy)<sub>m</sub>(solv)]<sup>3+</sup> (*m* = 1–3) were observed despite intensive ligand and solvent exchange processes. The tris(bipy) complex was crystallized as [Tl(bipy)<sub>3</sub>(dmsO)](ClO<sub>4</sub>)<sub>3</sub>(dmsO)<sub>2</sub> (**1**), and its crystal structure determined. In this compound, thallium is seven-coordinated; it is bonded to six nitrogen atoms of the three bipy molecules and to an oxygen atom of dmsO. Metal–metal bonded binuclear complexes [(NC)<sub>5</sub>Pt–Tl(CN)<sub>n</sub>(solv)]<sup>*n*–</sup> (*n* = 0–3) have been modified by attaching bipy molecules to the thallium atom. A reaction between [(NC)<sub>5</sub>Pt–Tl(dmsO)<sub>4</sub>](s) and 2,2'-bipyridine in dimethyl sulfoxide solution results in the formation of a new complex, [(NC)<sub>5</sub>Pt–Tl(bipy)(solv)]. The presence of a direct Pt–Tl bond in the complex is convincingly confirmed by a very strong one-bond <sup>195</sup>Pt–<sup>205</sup>Tl spin–spin coupling (<sup>1</sup>*J*(<sup>195</sup>Pt–<sup>205</sup>Tl) = 64.9 kHz) detected in both <sup>195</sup>Pt and <sup>205</sup>Tl NMR spectra. In solutions containing free cyanide, coordination of CN<sup>–</sup> to the thallium atom occurs, and the complex [(NC)<sub>5</sub>Pt–Tl(bipy)(CN)(solv)]<sup>–</sup> (<sup>1</sup>*J*(<sup>195</sup>Pt–<sup>205</sup>Tl) = 50.1 kHz) is formed as well. Two metal–metal bonded compounds containing bipy as a ligand were crystallized and their structures determined by X-ray diffraction: [(NC)<sub>5</sub>Pt–Tl(bipy)(dmsO)<sub>3</sub>] (**2**) and [(NC)<sub>5</sub>Pt–Tl(bipy)<sub>2</sub>] (**3**). The Pt–Tl bonding distances in the compounds, 2.6187(7) and 2.6117(5) Å, respectively, are among the shortest reported separations between these two metals. The corresponding force constants in the molecules, 1.38 and 1.68 N/cm, respectively, were calculated using Raman stretching frequencies of the Pt–Tl vibrations and are characteristic for a single metal–metal bond. Electronic absorption spectra were recorded for the [(NC)<sub>5</sub>Pt–Tl(bipy)<sub>m</sub>(solv)] compounds, and the optical transition was attributed to the metal–metal bond assigned.

### Introduction

Pt–Tl interaction and heterometallic metal–metal interactions in general are experiencing renewed interest in the literature.<sup>1</sup> This is to a large extent attributed to an increasing attention to the closed-shell metal–metal contacts appearing in the compounds of heavy, late transition and main group metals.<sup>2</sup> In the case of Pt–Tl compounds, such metallophilic

forces have been recognized in a number of systems where Tl<sup>I</sup>, a 6s<sup>2</sup> ion, is aggregating with various Pt<sup>0</sup> (5d<sup>10</sup>) or Pt<sup>II</sup> (5d<sup>8</sup>) centers (see refs 1a,b and references therein).

Recently, we have reported the synthesis and a structural study of a new family of binuclear platinum–thallium compounds with an unsupported and short metal–metal bond, [(NC)<sub>5</sub>Pt–Tl(CN)<sub>n</sub>(aq)]<sup>*n*–</sup> (*n* = 0–3), obtained from the reaction between platinum(II) tetracyano and thallium(III) cyano complexes.<sup>3</sup> Because of the fact that Tl<sup>III</sup> is not a closed-shell ion (s<sup>0</sup> rather than d<sup>10</sup> configuration<sup>2</sup>), bonding in the Pt<sup>II</sup>–Tl<sup>III</sup> entity is much stronger compared to weak,

\* Author to whom correspondence should be addressed. E-mail: Julius@inorg.kth.se.

<sup>†</sup> Arrhenius Laboratory, Department of Structural Chemistry, Stockholm University, S-10 691 Stockholm, Sweden.

<sup>‡</sup> Permanent address: Department of Chemistry, Shanxi University, 030006 Taiyuan, Shanxi Province, People's Republic of China.

<sup>§</sup> IFM-Department of Chemistry, Linköping University, SE-581 83 Linköping, Sweden.

(1) (a) Catalano, V. J.; Bennett, B. L.; Muratidis, S.; Noll, B. C. *J. Am. Chem. Soc.* **2001**, *123*, 173. (b) Janzen, M. C.; Jennings, M. C.; Puddephatt, R. J. *Inorg. Chem.* **2001**, *40*, 1728. (c) Gade, L. H. *Angew. Chem., Int. Ed.* **2001**, *40*, 3573.

(2) Pykkö, P. *Chem. Rev.* **1997**, *97*, 597.

(3) (a) Berg, K.; Glaser, J.; Read, M. C.; Tóth, I. *J. Am. Chem. Soc.* **1995**, *117*, 7550. (b) Maliarik, M.; Berg, K.; Glaser, J.; Sandström, M.; Tóth, I. *Inorg. Chem.* **1998**, *37*, 2910. (c) Jalilvand, F.; Glaser, J.; Maliarik, M.; Mink, J.; Persson, I.; Persson, P.; Sandström, M.; Tóth, I. *Inorg. Chem.* **2001**, *40*, 3889. (d) Jalilvand, F.; Eriksson, L.; Glaser, J.; Maliarik, M.; Mink, J.; Sandström, M.; Tóth, I.; Tóth, J. *Chem.–Eur. J.* **2001**, *7*, 2167.

attractive interaction in the  $\text{Pt}^0\text{--Tl}^{\text{I}}$  and  $\text{Pt}^{\text{II}}\text{--Tl}^{\text{I}}$  systems. The parameters of the Pt–Tl bond, such as interatomic distances, force constants, and spin–spin coupling constants  $^1J(^{195}\text{Pt}\text{--}^{205}\text{Tl})$ , indicate the presence of a single, polar covalent bond between the metal atoms in the family of compounds.<sup>3b,c</sup> Recently, the complexes have been subjected to a series of theoretical studies aimed at reproducing the vibrational frequencies, spin–spin coupling constants, and Pt–Tl separations and elucidating the nature of the metal–metal bond in the species.<sup>4</sup> The computed complexes and characteristics of the metal–metal bond are fully compatible with the experimental data and the proposed structures of the species.

Upon irradiation into the metal-to-metal charge-transfer absorption band, the compounds undergo photoinduced two-electron-transfer reactions between the coupled metals, giving rise to various complexes of platinum(IV) and monovalent thallium.<sup>5</sup> Possible photoelectrochemical applications of the compounds are limited because the absorption occurs only in the UV region and the electron transfer is not reversible. To shift the absorption into the visible range and to improve the light-absorption and the redox characteristics, the complexes should be modified while the Pt–Tl entity is kept intact. This can be done, e.g., by substituting the cyano ligands or by changing the solvent medium. To this end, it has been found that the platinum pentacyano unit in the Pt–Tl complexes is inert toward all tested competing ligands, whereas the thallium “part” of the species can be modified significantly. Different halide and pseudo-halide (F, Cl, Br, I, NCS)<sup>6a</sup> or molecular (en)<sup>6b</sup> ligands, as well as chromophore molecules or groups (bipy, phen,<sup>6c</sup> porphyrins<sup>6a</sup>), can be linked to the thallium atom in the  $[(\text{NC})_5\text{Pt}\text{--Tl}(\text{L})_m]$  (L = ligand) complexes, which allows their optical and photoredox properties to be tuned. In this paper we present the first results of modification of the coordination environment of the thallium atom in the bimetallic Pt–Tl compounds by means of the molecular 2,2′-bipyridine ligand; the speciation of the complexes was studied in the dimethyl sulfoxide solution.

Some adducts of thallium(III) with 2,2′-bipyridine, containing from one to three bipy ligands and halide, pseudo-halide, or nitrate ions, have been reported in the literature.<sup>7</sup> The suggested structures of the complexes  $\text{TiX}_3\cdot\text{bipy}$  and  $\text{TiX}_3\cdot 2\text{bipy}$  (X = halide) were based only on the results of conductivity and molecular weight measurements. Thus, for

the adduct of  $\text{TiX}_3\cdot\text{bipy}$ , both an ionic,  $[\text{TiX}_2(\text{bipy})_2]^+[\text{TiX}_4]^-$ , and a molecular structure were proposed to exist in nitrobenzene or acetonitrile, respectively.<sup>7c</sup> The only established crystal structure of the thallium(III) compound with 2,2′-bipyridine is  $[\text{Tl}(\text{bipy})_2(\text{NO}_3)_3]$ , where thallium is eight-coordinated and one of the nitrate groups is bidentate.<sup>8</sup> Equilibria in aqueous solutions of Tl–bipy complexes were studied by potentiometric and extraction methods, and the stepwise stability constants of the species  $\text{Tl}(\text{bipy})_m^{3+}$  ( $m = 1\text{--}3$ ) were determined to be  $2.5 \times 10^9$ ,  $5.0 \times 10^6$ , and  $5 \times 10^4$ , respectively.<sup>7b</sup>

In the present paper the interest is focused on the modification of the Pt–Tl compounds via complex formation between thallium(III) and 2,2′-bipyridine. The study was performed both for thallium(III) alone (in dimethyl sulfoxide solution and in the crystal structure of its tris(bipyridine) complex **1**) and for thallium bound in binuclear platinum–thallium compounds containing an unsupported metal–metal bond  $[(\text{NC})_5\text{Pt}\text{--Tl}(\text{bipy})_m(\text{solv})]$  (in dmsO solution and in two crystal structures containing mono(bipyridine) (**2**) and bis(bipyridine) (**3**) entities, respectively).

Throughout the text, the following notation is used for the composition of the complexes: the number of coordinated ligands is denoted by  $(\text{CN})_n$  ( $n = 0\text{--}3$ ) and  $(\text{bipy})_m$  ( $m = 0\text{--}3$ ), and  $-\text{Tl}(\text{bipy})_m(\text{solv})$  and  $-\text{Tl}(\text{solv})$  are used for an unknown solvation number of the metal entities.

## Experimental Section

**Materials and Synthesis. Preparation of Solutions.** A concentrated (1.2 M) aqueous solution of  $\text{Tl}(\text{ClO}_4)_3$  in 4.9 M  $\text{HClO}_4$  was obtained by anodic oxidation of  $\text{TlClO}_4$  and analyzed as described previously.<sup>9</sup> A dimethyl sulfoxide solution of  $[\text{Tl}(\text{dmsO})_6]^{3+}$  was obtained by dissolving solid  $[\text{Tl}(\text{dmsO})_6](\text{ClO}_4)_3$  in dmsO.<sup>10</sup> A dimethyl sulfoxide solution of  $[(\text{NC})_5\text{Pt}\text{--Tl}(\text{solv})]$  was prepared by reacting  $[\text{Tl}(\text{dmsO})_6](\text{ClO}_4)_3$  and  $\text{K}_2\text{Pt}(\text{CN})_4$  with a Tl/Pt molar ratio of 1/1 in the presence of a stoichiometric amount of NaCN in dimethyl sulfoxide.<sup>6b</sup>

**Preparation of Solid Compounds.  $[\text{Tl}(\text{bipy})_3(\text{dmsO})](\text{ClO}_4)_3\text{--}(\text{dmsO})_2$  (**1**).** A 0.5 g (3.2 mmol) sample of 2,2′-bipyridine was dissolved in 10 mL of methanol, and 0.8 mL of a 1.2 M aqueous solution of  $\text{Tl}(\text{ClO}_4)_3$  (1 mmol) was slowly added under continuous stirring at ambient temperature. A white precipitate was immediately formed. The precipitate was filtered, washed with methanol, and dried in a vacuum desiccator over silica gel until a constant mass was obtained. The solid was dissolved in dimethyl sulfoxide, and the solvent was slowly evaporated in a vacuum desiccator over silica gel. Colorless irregular platelike crystals of  $[\text{Tl}(\text{bipy})_3(\text{dmsO})](\text{ClO}_4)_3(\text{dmsO})_2$  were formed. The Raman band positions ( $\text{cm}^{-1}$ ) and assignments are as follows: 2918s ( $\text{CH}_3$  str); 1599vs, 1568m, 1497s, 1434m, 1312vs, 1065s, 1024vs (characteristic bands of bipy); 930s ( $\text{ClO}_4^-$  str), 656s (CS str); 456s, 403w, 363s, 246m, 232m (TlN and TlO str, TlNC, TlOS, CSC, and OSC bend). The abbreviations are vs = very strong, s = strong, m = medium, w =

(4) (a) Autschbach, J.; Ziegler, T. *J. Am. Chem. Soc.* **2001**, *123*, 5320. (b) Russo, M. R.; Kaltsoyannis, N. *Inorg. Chim. Acta* **2001**, *312*, 221. (c) Autschbach, J.; Le Guennic, B. *J. Am. Chem. Soc.* **2003**, *125*, 13585.

(5) (a) Maliarik, M.; Glaser, J.; Tóth, I. *Inorg. Chem.* **1998**, *37*, 5452. (b) Maliarik, M. Compounds with Non-Butressed Metal–Metal Bond between Platinum and Thallium. Model Systems for Photoinduced Two-Electron-Transfer. Ph.D. Thesis, Royal Institute of Technology, Stockholm, 2001 (<http://media.lib.kth.se:8080/dissengin.asp>, select “Department of Chemistry”).

(6) (a) Ma, G.; Maliarik, M.; Glaser, J. Unpublished results from this laboratory. (b) Ma, G.; Kritikos, M.; Glaser, J. *Eur. J. Inorg. Chem.* **2001**, 1311. (c) Ma, G.; Fischer, A.; Glaser, J. *Eur. J. Inorg. Chem.* **2002**, 1307.

(7) (a) Sutton, G. J. *Aust. J. Chem.* **1958**, *11*, 120. (b) Kul’ba, F. Y.; Mironov, V. E. *The Chemistry of Thallium*; Goskhimizdat: Leningrad, 1963. (c) Lee, A. G. *The Chemistry of Thallium*; Elsevier: Amsterdam, 1971.

(8) Musso, S. Untersuchung von Gleichgewichten in wässriger Lösung und Kristallstrukturbestimmung von Komplexen des Thalliums(III) mit Chelatliganden. Ph.D. Thesis, ETH, Zurich, Switzerland, 1993.

(9) (a) Biedermann, G. *Ark. Kemi* **1953**, *5*, 441. (b) Blixt, J.; Györi, B.; Glaser, J. *J. Am. Chem. Soc.* **1989**, *111*, 7784.

(10) Ma, G.; Molla-Abbassi, A.; Kritikos, M.; Ilyukhin, A.; Kessler, V.; Skripkin, M.; Sandström, M.; Glaser, J.; Näslund, J.; Persson, I. *Inorg. Chem.* **2001**, *40*, 6432.

weak, str = stretching. Anal. Calcd for  $C_{36}H_{41}Cl_3N_6O_{15}S_3Tl$ : C, 36.05; H, 3.65; N, 6.95; S, 7.85. Found: C, 35.86; H, 3.40; N, 6.97; S, 7.97.

The solid compounds  $[Tl(dms)_6](ClO_4)_3$ ,<sup>10</sup>  $(NC)_5Pt$ ,<sup>3b,d</sup> and  $[(NC)_5Pt-Tl(dms)_4]^{6b}$  were obtained as described previously.

$[(NC)_5Pt-Tl(bipy)(dms)_3]$  (**2**). A 0.012 g (0.077 mmol) sample of 2,2'-bipyridine was dissolved in 3 mL of water, and 0.039 g (0.073 mmol) of the solid compound  $(NC)_5Pt$  was slowly added to the solution upon continuous stirring at ambient temperature. Formation of another, white and barely soluble solid phase, with the composition best described as  $[(NC)_5Pt-Tl(bipy)(H_2O)_3]$ , was observed. The heterogeneous mixture was stirred for 5 h. The white precipitate was filtered and dried in a vacuum desiccator over silica gel until a constant mass was reached. Anal. Calcd for  $C_{15}H_{14}N_7O_3-PtTl$ : C, 24.32; H, 1.89; N, 13.20. Found: C, 25.03; H, 1.83; N, 13.20. The solid was dissolved in dimethyl sulfoxide. The solvent was slowly evaporated in a vacuum desiccator over silica gel. Colorless rod-shaped crystals were formed. Raman band positions ( $cm^{-1}$ ) and assignments: 2995m, 2915s ( $CH_3$  str); 2188s ( $C\equiv N^A$  str); 2178m, 2164m ( $C\equiv N^C$  str); 1590vs, 1568s, 1491s, 1425m, 1308vs, 1063s, 1016m (characteristic bands of bipy); 674s (CS str); 461s, 435m, 385vs, 357s, 309m, 260m (TIN and TIO str, TINC, TIOS, CSC, and OSC bend); 153vs (Pt-Tl str). Anal. Calcd for  $C_{21}H_{26}N_7O_3S_3PtTl$ : C, 27.39; H, 2.83; N, 10.65; S, 10.44. Found: C, 27.55; H, 3.10; N, 10.40; S, 10.45.

$[(NC)_5Pt-Tl(bipy)_2]$  (**3**). The solid compounds  $[Tl(bipy)_3(dms)_2](ClO_4)_3(dms)_2$  (0.05 mmol) and  $K_2Pt(CN)_4$  (0.05 mmol) were dissolved in dimethyl sulfoxide, and 0.1 mL of a 0.5 M solution of NaCN in dms was slowly added to the mixture with continuous stirring at ambient temperature.<sup>11</sup> The solvent was slowly evaporated in a vacuum desiccator over silica gel. Yellow cube-shaped crystals were formed. Raman band positions ( $cm^{-1}$ ) and assignments: 2186s ( $C\equiv N^A$  str); 2176m, 2163m ( $C\equiv N^C$  str); 1594vs, 1566m, 1495m, 1433m, 1310vs, 1067s, 1018vs (characteristic bands of bipy); 458m, 397m, 356s, 249m (TIN str, TINC bend); 169vs (Pt-Tl str). Anal. Calcd for  $C_{25}H_{16}N_9PtTl$ : C, 35.63; H, 1.90; N, 14.96. Found: C, 35.38; H, 1.85; N, 14.52.

*Warning! Although no problem was experienced with the present samples, perchlorates in organic solvents are potentially dangerous. The toxicity of thallium and its compounds has been previously discussed.*<sup>12</sup>

**Methods and Measurements. NMR Measurements.** All NMR measurements were performed on a Bruker DMX500 spectrometer at a probe temperature of 298 ( $\pm 0.5$ ) K. For  $^{13}C$  and  $^1H$  NMR measurements, solutions were prepared in DMSO- $d_6$ , and some in  $CD_3CN$ . Information on typical  $^{205}Tl$ ,  $^{195}Pt$ , and  $^{13}C$  NMR parameters for similar systems has been given in recent papers from this laboratory.<sup>3b</sup>

**Vibrational Spectroscopy.** Raman spectra were measured using a Renishaw System 1000 spectrometer, equipped with a Leica DMLM microscope, a 25 mW diode laser (780 nm), and a Peltier-cooled CCD detector. Raman spectra were also measured by means of the FT-Raman accessory of a Bio-RAD FTS 6000 FT-IR

**Table 1.** Selected Crystal Data for  $[Tl(bipy)_3(dms)_2](ClO_4)_3(dms)_2$  (**1**),  $[(NC)_5Pt-Tl(bipy)(dms)_3]$  (**2**), and  $[(NC)_5Pt-Tl(bipy)_2]$  (**3**)<sup>a</sup>

	1	2	3
empirical formula	$C_{36}H_{42}Cl_3N_6O_{15}S_3Tl$	$C_{21}H_{26}N_7O_3S_3TlPt$	$C_{25}H_{16}N_9PtTl$
fw	1205.69	920.16	841.93
cryst syst	monoclinic	monoclinic	monoclinic
space group	$P2_1/c$ (No. 14)	$P2_1/n$ (No. 14)	$I2/a$ (No. 15)
<i>a</i> , Å	10.923(1)	9.4293(9)	15.943(2)
<i>b</i> , Å	36.522(4)	17.335(2)	9.6982(8)
<i>c</i> , Å	12.026(1)	18.284(2)	16.452(2)
$\beta$ , deg	90.08(2)	104.48(2)	98.98(2)
<i>V</i> , Å <sup>3</sup>	4797.9(9)	2893.6(6)	2512.5(5)
<i>Z</i>	4	4	4
$\rho_{calcd}$ , g cm <sup>-3</sup>	1.670(1)	2.112(1)	2.226(1)
Temp, K	243(1)	150(1)	293(1)
$\mu$ (Mo K $\alpha$ ), mm <sup>-1</sup>	3.733	10.64	12.00
<i>F</i> (000)	2400.0	1728.0	1552.0
<i>N</i> (obsd)	5976	2859	1443
<i>R1</i> , w <i>R2</i> ( <i>I</i> > 2 $\sigma$ ( <i>I</i> ))	0.0447, 0.1264	0.0423, 0.0794	0.0187, 0.0417
$\Delta\rho_{max}$ , $\Delta\rho_{min}$ (e/Å <sup>3</sup> )	1.107, -2.064	2.044, -2.852	1.001, -0.916

<sup>a</sup> *R* values are defined as  $R1 = \sum |F_o| - |F_c| / \sum |F_o|$  and  $wR2 = [\sum (w(F_o^2 - F_c^2)^2) / \sum (w(F_o^2)^2)]^{1/2}$ .

spectrometer. The 1024 nm line from a Spectra-Physics Nd:YAG laser was used to irradiate the sample with about 150 mW.

**UV-Vis Measurements.** All spectra were obtained using a Varian Cary-5 spectrophotometer. Measurements were carried out at ambient temperature. Silica cuvettes with 0.1 cm path lengths were used.

**Crystal Structure Determination.** Suitable single crystals of **1-3** were selected and mounted on glass fibers with epoxy glue. Single-crystal X-ray diffraction data were collected on a Stoe image-plate diffractometer. Selected crystallographic and experimental data for **1-3** together with the refinement details are given in Table 1. Systematic absences in the collected diffraction data were consistent with space groups  $P2_1/c$  (No. 14),  $P2_1/n$  (No. 14), and  $I2/a$  (No. 15) for **1-3**, respectively. The data were corrected for Lorentz, polarization, and absorption effects using the X-Shape program package.<sup>13a</sup> The structures were solved using direct methods and refined against  $F^2$  using the computer programs SHELXS86<sup>13b</sup> and SHELXL97,<sup>13c</sup> respectively. All non-hydrogen atoms were refined anisotropically. Hydrogen atoms were added at ideal positions and refined using a riding model. For **1**, the S3 atom in one of the solvated dms molecules was treated as disordered over two sites with equal occupancy. One of the perchlorate anions showed rotational disorder. This disorder was modeled as two partially occupied tetrahedral  $ClO_4$  units were the site occupation factors of the two units added to unity. Moreover, for **1** the diffraction data indicated orthorhombic symmetry. However, in this higher symmetry ( $Pnma$ ) the solvated dms groups could not be satisfactorily refined.

## Results and Discussion

**$Tl^{3+}$ -bipy Speciation in Dimethyl Sulfoxide Solution.  $[Tl(bipy)_m(soln)]^{3+}$  ( $m = 1-3$ ) Complexes.** Complex formation between thallium(III) cation and 2,2'-bipyridine in solution was previously studied in an aqueous medium.<sup>14</sup>

- (11) Fast reaction between colorless dimethyl sulfoxide solutions of  $[Tl(bipy)_3(dms)_2](ClO_4)_3(dms)_2$  and  $K_2Pt(CN)_4$  results in immediate yellow coloration of the solution. The strong absorption band at 350 nm observed in the UV-vis spectrum of the solution is attributed to an MMCT transition in the complex  $[(NC)_4Pt-Tl(bipy)_2]^{3+}$ . The complex then reacts slowly with free cyanide ion, which results in continuous degradation of the band and shifting of the absorption to lower wavelengths. A study of a family of  $[(NC)_4Pt-Tl(L)_n(soln)]^{3+}$  species is outside the scope of this paper, to be published.
- (12) Glaser, J. In *Advances in Inorganic Chemistry*; Sykes, A. J., Ed.; Academic Press: San Diego, 1995; Vol. 43, p 1.

- (13) (a) *STOE, X-SHAPE revision 1.09. Crystal Optimisation for Numerical Absorption Correction*; STOE Company: Darmstadt, Germany, 1997. (b) Sheldrick, G. M. *Acta Crystallogr.* **1994**, *A46*, 467. (c) Sheldrick, G. M. *SHELXL97. Computer Program for the Refinement of Crystal Structures*, Release 97-2; University of Göttingen: Göttingen, Germany, 1997.
- (14) (a) Kul'ba, F. Y.; Makashev, Y. A.; Mironov, V. E. *Zh. Neorg. Khim.* **1961**, *6*, 630. (b) Kul'ba, F. Y.; Makashev, Y. A. *Zh. Neorg. Khim.* **1962**, *7*, 689. (c) Kul'ba, F. Y.; Makashev, Y. A. *Zh. Neorg. Khim.* **1962**, *7*, 1280.

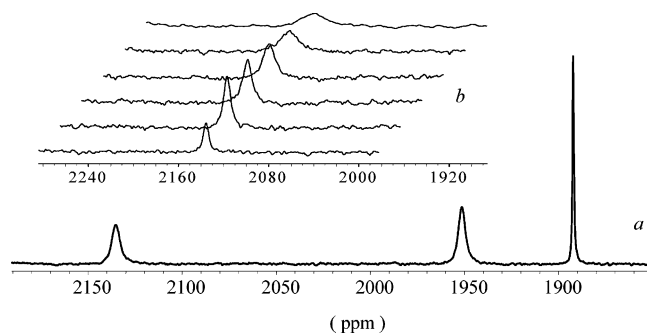


**Figure 1.**  $^{205}\text{Tl}$  NMR spectra of  $[\text{Tl}(\text{dmsO})_6]^{3+}$ -bipy solutions in dmsO ( $C_{\text{Tl}^{III}} = 25 \text{ mM}$ ): (a)  $C_{\text{bipy}} = 15 \text{ mM}$ ; (b) the bipy concentration is increased continuously in the range 28–144 mM (from bottom to top).

Stability constants and thermochemical characteristics were determined for the three complexes  $\text{Tl}(\text{bipy})_m^{3+}$  ( $m = 1-3$ ). The structural information on the complexes is limited to the number of bipy ligands coordinated to thallium, while the solvation of the metal cation and the geometry of the species have been neither studied nor discussed. A conductometric study of the complexes  $\text{TlX}_3 \cdot \text{bipy}$  and  $\text{TlX}_3 \cdot 2\text{bipy}$  ( $X = \text{halide}$ ), carried out in nitrobenzene and acetonitrile solutions, focused on determination of the composition of the solid compounds.<sup>7c</sup> In nitrobenzene, a solvent with a weak coordinating ability (donor number (DN) = 4.4),<sup>15</sup> an ionic structure of the compound  $\text{TlX}_3 \cdot \text{bipy}$  ( $[\text{TlX}_2(\text{bipy})_2]^+[\text{TlX}_4]^-$ ) was proposed. On the contrary, when the compounds were dissolved in the more strongly coordinating N-donor solvent acetonitrile (DN = 14.1),<sup>15</sup> the solutions behaved as weak electrolytes. This was interpreted in terms of formation of neutral molecules, where acetonitrile fills coordination vacancies in the thallium polyhedron. Thus, it can be expected that dimethyl sulfoxide (DN = 29.8)<sup>15</sup> will behave as a stronger competing ligand for the complex formation in the  $\text{Tl}^{3+}$ -bipy-dmsO system.

In the  $^{205}\text{Tl}$  NMR spectrum of a solution of  $[\text{Tl}(\text{dmsO})_6](\text{ClO}_4)_3(\text{s})$  in dmsO only one signal is observed, which belongs to the species  $[\text{Tl}(\text{dmsO})_6]^{3+}$  ( $\delta = 1891 \text{ ppm}$ ,  $\Delta H_{1/2} = 80 \text{ Hz}$ ). When 2,2'-bipyridine is added to this solution ( $C_{\text{Tl}} = 0.025 \text{ M}$ , molar ratio  $\text{bipy}/\text{Tl} = 0.2$ ), a new broad signal ( $\Delta H_{1/2} = 1130 \text{ Hz}$ ) appears at 1951 ppm. Upon further increase of the concentration of bipy ( $0.2 < \text{bipy}/\text{Tl} < 2.0$ ) a signal at 2134 ppm ( $\Delta H_{1/2} = 1200 \text{ Hz}$ ) appears in the  $^{205}\text{Tl}$  NMR spectra, accompanied by a gradual decrease of the intensity of the signals at 1891 and 1951 ppm (Figure 1a). Taking into account the known concentrations of thallium and 2,2'-bipyridine in the solution and the integral intensities of the signals, these resonances can be attributed to thallium species with coordinated bipy,  $[\text{Tl}(\text{bipy})(\text{solv})]^{3+}$  and  $[\text{Tl}(\text{bipy})_2(\text{solv})]^{3+}$ .

The substantial broadening of the signals, as compared to that of  $[\text{Tl}(\text{dmsO})_6]^{3+}$ , results probably from a combined effect of the interaction with the quadrupolar nitrogen nuclei of the coordinated bipy ligand and ligand exchange processes (cf. the discussion below).<sup>16</sup> No other signals have been detected in the  $^{205}\text{Tl}$  NMR spectra for the studied range of

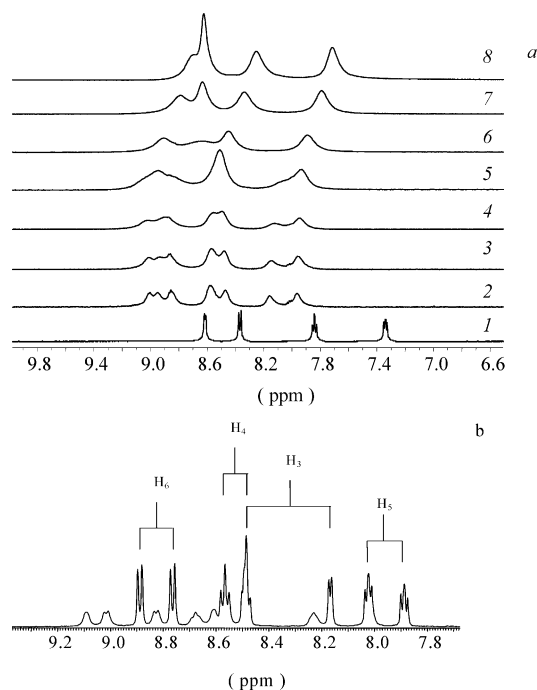


**Figure 2.**  $^1\text{H}$  NMR spectra (a bipy chemical shift region) of  $[\text{Tl}(\text{dmsO})_6]^{3+}$ -bipy solutions in (a)  $\text{DMSO}-d_6$ ,  $C_{\text{Tl}^{III}} = 0$  (solution 1) and 50 mM (solutions 2–8) mM,  $C_{\text{bipy}} = 9$  (solution 2), 25 (solution 3), 50 (solution 4), 100 (solution 5), 150 (solution 6), 200 (solution 7), and 250 (solution 8) mM and (b)  $\text{CD}_3\text{CN}$ , 50 mM  $[\text{Tl}(\text{bipy})_3(\text{dmsO})](\text{ClO}_4)_3(\text{dmsO})_2$ ; only thallium-coupled signals belonging to the tris(bipy) species are marked.

molar ratios (up to  $\text{bipy}/\text{Tl} = 7.0$ ). An increase of the ratio over 2.0 results in the disappearance of all signals in the spectra, except for the one at 2134 ppm. The line width of the latter increases substantially and finally, at  $\text{bipy}/\text{Tl} > 6.0$ , is broadened beyond detection (Figure 1b).

Coordination of the 2,2'-bipyridine molecules to the thallium(III) ion in the complexes  $[\text{Tl}(\text{bipy})_m(\text{solv})]^{3+}$  is further supported by  $^1\text{H}$  and  $^{13}\text{C}$  NMR spectra. Thus, for solutions with  $\text{bipy}/\text{Tl} \leq 0.2$ ,  $^1\text{H}$  signals of all four groups of protons of bipy are shifted to higher frequency compared to the signals of bipy in dmsO solution (Figure 2a, spectrum 2). The signals are very broad ( $\Delta H_{1/2} = \sim 30 \text{ Hz}$ ), which prevents the observation of  $^1\text{H}$ - $^1\text{H}$  spin-spin coupling; on the other hand, the coupling of the bipy protons to thallium could be detected at low bipy concentration (see the Supporting Information, Figure S1a). The  $^1\text{H}$  and  $^{13}\text{C}\{^1\text{H}\}$  chemical shifts of the signals and the values of  $J(\text{H}-\text{Tl})$  and  $J(\text{C}-\text{Tl})$  (see the Supporting Information, Figure S1b) are presented in Table 2. Both the  $^{13}\text{C}$  chemical shifts of the signals and the C-Tl coupling constants are in agreement with the values reported for bipy in  $[\text{Tl}(\text{edta})(\text{bipy})]^-$  in aqueous solution.<sup>8</sup> These findings allowed for the assignment of the new signals appearing in the  $^1\text{H}$  and  $^{13}\text{C}$  NMR spectra to a mono(bipy) thallium species solvated by dmsO:  $[\text{Tl}(\text{bipy})(\text{solv})]^{3+}$ .

In contrast to  $^{205}\text{Tl}$  NMR, in the corresponding  $^1\text{H}$  and  $^{13}\text{C}$  spectra separate signals of mono- and bis(bipy) complexes have not been observed. Upon an increase of bipy

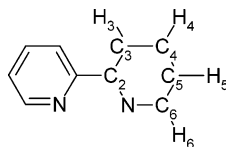
(15) Gutmann, V. *The Donor-Acceptor Approach to Molecular Interactions*; Plenum Press: New York and London, 1978.

(16) A detailed study of the exchange dynamics in the Tl-bipy-S (S (solvent) = dmsO,  $\text{CH}_3\text{CN}$ ) system is outside the scope of this paper.

**Table 2.**  $^1\text{H}$ ,  $^{13}\text{C}$ , and  $^{205}\text{Tl}$  NMR Data (Chemical Shifts (ppm) and  $^1\text{H}/^{13}\text{C}$ –Tl Spin–Spin Coupling Constants (Hz)) of 2,2'-Bipyridine (bipy) and  $[\text{Tl}(\text{bipy})_m(\text{solv})]^{3+}$  in Dimethyl Sulfoxide and Acetonitrile Solution<sup>a,b</sup>

	Tl	$\text{C}_2/{}^2J$	$\text{C}_3/{}^3J$	$\text{C}_4/{}^4J$	$\text{C}_5/{}^5J$	$\text{C}_6/{}^2J$	$\text{H}_3/{}^4J$	$\text{H}_4/{}^5J$	$\text{H}_5/{}^4J$	$\text{H}_6/{}^3J$
2,2'-bipyridine in dmsO		155.1	124.1	137.2	120.3	149.1	8.3	7.9	7.4	8.6
2,2'-bipyridine in $\text{CH}_3\text{CN}$		156.8	124.9	138.0	121.6	150.2	8.4	7.9	7.4	8.7
$[\text{Tl}(\text{bipy})(\text{solv})]^{3+}$ in dmsO	1951	143.0/355	129.0/131	143.8/49	124.5/175	149.2/42	8.8/139	8.6/52	8.1/94	9.0/30
$[\text{Tl}(\text{bipy})_2(\text{solv})]^{3+}$ in dmsO	2134									
$[\text{Tl}(\text{bipy})_2(\text{solv})]^{3+}$ in $\text{CH}_3\text{CN}^c$	2530	144.6/363	126.1/193	145.7/53	130.7/161	149.6/102	8.9/242	8.6/56	8.1/103	8.9/95
$[\text{Tl}(\text{bipy})_3(\text{solv})]^{3+}$ in $\text{CH}_3\text{CN}^c$	2664	146.1/253	127.0/127	145.7/41	130.7/112	150.1/84	8.3/159	8.5/40	8.0/69	8.8/62

<sup>a</sup> The notation of the proton and carbon atoms of the bipy ligand is presented below. <sup>b</sup> Chemical shifts of  $^1\text{H}$  and  $^{13}\text{C}$  signals are given in parts per million relative to the signals of  $\text{DMSO}-d_6$  and acetonitrile- $d_3$  solvents at 2.49 and 39.5 ppm and 1.96 and 1.3 ppm, respectively, calibrated by the corresponding signals of TMS. <sup>c</sup> The solvation numbers were not determined.



coordination the  $^1\text{H}$  signals are further broadened, compared to those of  $[\text{Tl}(\text{bipy})(\text{solv})]^{3+}$ , and overlap strongly (Figure 2a). No spin–spin coupling to the thallium can be observed any longer, and at bipy/Tl = 2.0 only four poorly resolved lines are detected in proton spectra, somewhat shifted to low frequency compared to the mono species (Figure 2a, spectrum 5). Similarly, the  $^{13}\text{C}$  NMR spectra show only a set of four broad signals with no  $^{13}\text{C}$ –Tl splitting.<sup>17,18</sup> Neither in  $^1\text{H}$  nor in  $^{13}\text{C}$  spectra have signals belonging to 2,2'-bipyridine of the tris(bipy) complex been observed. In both cases a continuous shift of the signals to lower frequency occurs (cf., e.g., Figure 2a, solutions 6–8). No signal of free, noncoordinated bipy can be observed at a higher excess of the ligand (bipy/Tl  $\geq$  3). At bipy/Tl > 5, two signals in the proton spectra collapse into one, and only three lines can be detected.

Although the subject of this work is the study of Tl–bipy speciation in dmsO, to obtain information on the tris(bipy) complex, a comparative study of the  $[\text{Tl}(\text{bipy})_m(\text{solv})]^{3+}$  species in another solvent, namely, acetonitrile, has also been carried out. In contrast to the Tl–bipy–dmsO system, dissolution of the solid  $[\text{Tl}(\text{bipy})_3(\text{dmsO})(\text{ClO}_4)_3(\text{dmsO})_2]$  in acetonitrile allows separate and much narrower (e.g.,  $\Delta H_{1/2} \leq 280$  Hz in  $^{205}\text{Tl}$  NMR spectra) signals of both tris- and bis(bipy) complexes of thallium to be observed in the  $^{205}\text{Tl}$ ,  $^1\text{H}$ , and  $^{13}\text{C}$  NMR spectra (Figure 2b, Table 2; see also the Supporting Information, Figure S2).<sup>19</sup> An increase of the bipy concentration shifts the equilibrium to the tris(bipy) species.

In contrast to the Tl–bipy systems, both  $^1\text{H}$  and  $^{13}\text{C}$  NMR spectra of 2,2'-bipyridine in dimethyl sulfoxide and in acetonitrile are almost identical in terms of the chemical shifts of the signals, their line widths, and the values of the  $^1\text{H}$ – $^1\text{H}$  spin–spin coupling (Table 2). Thus, a pronounced solvent dependence of the  $[\text{Tl}(\text{bipy})_3]^{3+}$  species cannot be attributed

to the physical properties of the medium: viscosity, dielectric constant, dipole moment, etc. Instead, it is related to the coordinating features of the solvent molecules in the thallium complexes with bipy. It can be supposed that because of the much stronger donor ability of the dmsO ligand (DN = 29.8), compared to  $\text{CH}_3\text{CN}$  (DN = 14.1),<sup>15</sup> the former has enough capacity to compete with the bipy ligand and is still coordinated to the thallium atom even in the tris(bipy) complex. Coordination of three bipy ligands labilizes the Tl–O (dmsO) bonding, which would probably lead to an intensified exchange between the coordinated dimethyl sulfoxide in the tris- and bis(bipy) compounds. The solvent exchange is fast on the  $^{205}\text{Tl}$  NMR time scale, which broadens the  $[\text{Tl}(\text{bipy})_3(\text{solv})]^{3+}$  signal beyond detection, while in the case of  $^1\text{H}$  and  $^{13}\text{C}$  NMR it averages the corresponding signals of the bis- and tris(bipy) species.

Conversely, no solvent coordination to the  $[\text{Tl}(\text{bipy})_3]^{3+}$  complex probably occurs in the acetonitrile solution, which disables this exchange path and permits detection of this species separately, by means of  $^{205}\text{Tl}$ ,  $^1\text{H}$ , and  $^{13}\text{C}$  NMR spectra. When larger amounts of 2,2'-bipyridine are introduced to the  $[\text{Tl}(\text{bipy})_3]^{3+}$  solution in acetonitrile, similar to the dmsO case, no signals of free bipy appear in either  $^1\text{H}$  or  $^{13}\text{C}$  NMR. The signals of the coordinated ligand are shifted to lower frequencies, and the coupling to thallium is no longer observed. These results are interpreted in terms of an exchange of bipy between the coordinated and free ligand occurring in both dimethyl sulfoxide and acetonitrile solvents at higher bipy/Tl ratios.

The study of the complex formation between  $\text{Tl}^{3+}$  and 2,2'-bipyridine in nonaqueous media shows therefore a number of exchange processes occurring in the system. The exchange reactions are solvent-dependent. For the  $[\text{Tl}(\text{bipy})_m]^{3+}$  complexes in dimethyl sulfoxide they include an exchange of the solvent molecules among the solvated  $[\text{Tl}(\text{bipy})_m(\text{solv})]^{3+}$  species,  $[\text{Tl}(\text{dmsO})_6]^{3+}$ , and the bulk solvent. In addition, intensive exchange of the bipy ligands between the  $[\text{Tl}(\text{bipy})_m(\text{solv})]^{3+}$  complexes takes place in the range  $\sim 0.3 \leq \text{bipy/Tl} \leq \sim 3$ . At higher ligand concentrations a free bipy is involved in the exchange process. For the acetonitrile solutions only the latter case seems to be of importance.<sup>16</sup>

(17) The  $^1\text{H}$  signal of coordinated dmsO was observed for the dimethyl sulfoxide solutions of  $\text{Tl}(\text{CF}_3\text{SO}_3)_3$  and  $[\text{Tl}(\text{dmsO})_6](\text{ClO}_4)_3$  in the range 3.5–4.5 ppm, depending on the salt concentration.

(18) The signals of the  $\text{C}^2$  and  $\text{C}^4$  carbons of bipy coordinated to thallium have close values of chemical shift and collapse into one broad signal.

(19) As could be expected, the  $^{205}\text{Tl}$  NMR chemical shift of the solvated thallium(III) complexes is very sensitive to the change of solvent. Thus, the chemical shift of bis(bipy) species in acetonitrile is 2530 ppm compared to 2134 ppm in dimethyl sulfoxide.

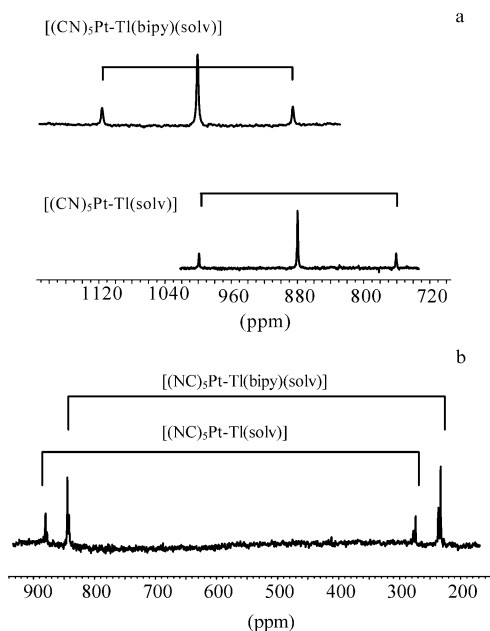


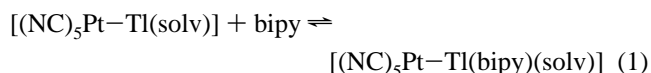
**Figure 3.**  $^{205}\text{Tl}$  (a) and  $^{195}\text{Pt}$  (b) NMR spectra of  $[(\text{NC})_5\text{Pt-Tl}(\text{solv})]$  and  $[(\text{NC})_5\text{Pt-Tl}(\text{bipy})(\text{solv})]$  complexes in dmsO solution. The Pt–Tl spin–spin coupling constants are indicated.

**Pt–Tl–bipy Speciation in Dimethyl Sulfoxide Solution.  $[(\text{NC})_5\text{Pt-Tl}(\text{bipy})_m(\text{solv})]$  ( $m = 1, 2$ ) and  $[(\text{NC})_5\text{Pt-Tl}(\text{bipy})(\text{CN})(\text{solv})]^-$  Complexes.** In a manner similar to that for cyano complexes  $[(\text{NC})_5\text{Pt-Tl}(\text{CN})_n(\text{aq})]^{n-}$  in an aqueous medium,<sup>3b,c</sup> two principal preparative routes can be used to obtain  $[(\text{NC})_5\text{Pt-Tl}(\text{bipy})_m(\text{solv})]$  complexes in dimethyl sulfoxide solution, namely, (1) a reaction between equimolar amounts of  $[\text{Pt}(\text{CN})_4]^{2-}$  and  $[\text{Tl}(\text{bipy})_m(\text{solv})]^{3+}$  ( $m = 1, 2$ ) in the presence of excess cyanide ( $[\text{CN}^-]_{\text{excess}}/[\text{M}] = 1/1$  ( $\text{M} = \text{Pt}, \text{Tl}$ )) in dimethyl sulfoxide solution,<sup>6c</sup> and (2) a reaction between crystalline  $[(\text{NC})_5\text{Pt-Tl}(\text{dmsO})_4]$  and 2,2'-bipyridine in dimethyl sulfoxide solution.<sup>20</sup>

Formation of the complex  $[(\text{NC})_5\text{Pt-Tl}(\text{solv})]$  in dimethyl sulfoxide solution was described in a recent paper from this laboratory.<sup>6b</sup> When 2,2'-bipyridine is added to this solution ( $\text{bipy}/\text{Tl} = 0.6$ ), a new group of signals (intensity ratio  $\sim 1/4/1$ ) centered at 1016 ppm ( $\Delta H_{1/2} = 270$  Hz) appears in the  $^{205}\text{Tl}$  NMR spectra in addition to the signal of  $[(\text{NC})_5\text{Pt-Tl}(\text{solv})]$  ( $\delta = 887$  ppm) (Figure 3a). Such a three-line pattern is characteristic of the binuclear Pt–Tl complexes and arises from the one-bond spin–spin coupling between the  $^{205}\text{Tl}$  and  $^{195}\text{Pt}$  nuclei ( $^{195}\text{Pt}$ ,  $I = 1/2$ , natural abundance 33.8%):  $^1J(^{205}\text{Tl}-^{195}\text{Pt}) = 64.9$  kHz (65.9 kHz for  $[(\text{NC})_5\text{Pt-Tl}(\text{solv})]$ ). The same value of the coupling constant can be obtained from the  $^{195}\text{Pt}$  NMR spectrum, which consists of two pairs of doublets with an intensity ratio of  $\sim 2.4$  within each doublet (due to the spin–spin coupling to the isotopomers of thallium,  $^{205}\text{Tl}$  and  $^{203}\text{Tl}$ , both  $I = 1/2$ , natural abundance 70.5% and 29.5%, respectively); the signal is centered at 539 ppm (574 ppm for  $[(\text{NC})_5\text{Pt-Tl}(\text{solv})]$ ) (Figure 3b).

(20) Similarly, the complexes can be obtained by reaction between the compound  $[(\text{NC})_5\text{Pt-Tl}(\text{s})]$  and 2,2'-bipyridine in aqueous solution, followed by the solid product being dissolved in dimethyl sulfoxide (cf. the Experimental Section).

When the reaction is carried out between 2,2'-bipyridine and the  $^{13}\text{C}$ -enriched  $[(\text{NC})_5\text{Pt-Tl}(\text{solv})]$ , both  $^{13}\text{C}$  and  $^{205}\text{Tl}$  NMR spectra clearly show that the pentacyanoplatinum unit is preserved in the bimetallic complex, with four equivalent CN ligands in an equatorial plane around platinum, and one CN occupying the axial position *trans* to the platinum–thallium bond (Table 3).<sup>21</sup> This leads to the conclusion that the only method of coordination of bipy to the complex is via the thallium atom, yielding dmsO-solvated mono(bipy) species:



In a manner similar to that in the case of the  $[\text{Tl}(\text{bipy})_m(\text{solv})]^{3+}$  complexes, the characterization of the coordinated bipy ligand in the bimetallic Pt–Tl species in dmsO solution by means of both  $^1\text{H}$  and  $^{13}\text{C}$  NMR is hampered by the ligand/solvent exchange processes. In all cases the spectra show four broad signals of the ligand in the range of 8.0–9.2 ppm ( $\Delta\nu_{1/2} = 30\text{--}80$  Hz) and 124–149 ppm ( $\Delta\nu_{1/2} = 30\text{--}55$  Hz) for  $^1\text{H}$  and  $^{13}\text{C}$ , respectively; no coupling of the nuclei to thallium could be detected.<sup>18</sup>

Further addition of 2,2'-bipyridine to the solution (up to  $\text{bipy}/\text{Tl} = 6$ ) does not lead to the appearance of new signals in the  $^{205}\text{Tl}$  NMR spectra. The intensity of the signal at 1016 ppm gradually decreases, while its line width increases substantially, and at  $\text{bipy}/\text{Tl} \geq 6$  the signal broadens beyond detection. No additional signals of the bimetallic Pt–Tl compounds could be detected by  $^{195}\text{Pt}$  NMR. The signals of the individual complexes could be distinguished neither in  $^1\text{H}$  nor in  $^{13}\text{C}$  NMR spectra: in the same way as for the monomeric thallium complexes described above, only four broad lines were observed in each case, and an increase of the bipy concentration resulted in a continuous shift of the signals to low frequency.

When additional cyanide ions are introduced into a dmsO solution of  $[(\text{NC})_5\text{Pt-Tl}(\text{bipy})(\text{solv})]$  up to a CN/Tl ratio of 1, a new platinum-coupled signal is detected in the  $^{205}\text{Tl}$  NMR spectrum at  $\delta_{\text{Tl}} = 1772$  ppm ( $^1J(^{205}\text{Tl}-^{195}\text{Pt}) = 50.1$  kHz). Both the signal intensities of the three-line pattern and the  $^{195}\text{Pt}$  NMR spectrum of the solution indicate that a binuclear Pt–Tl compound forms, while the  $^1\text{H}$  and  $^{13}\text{C}$  spectra show characteristic signals of the bipy ligand. When the complex is  $^{13}\text{C}$ -enriched, both its  $^{13}\text{C}$  and  $^{205}\text{Tl}$  spectra unambiguously point to the presence of one extra cyanide ligand,  $\text{C}^{\text{B}}$ , in the compound, directly bound to the thallium atom (Table 3 and the Supporting Information, Figure S3). Therefore, the composition of the species is  $[(\text{NC})_5\text{Pt-Tl}(\text{bipy})(\text{CN})(\text{solv})]^-$ .

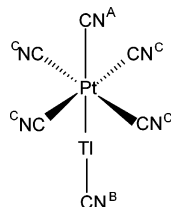
The same complex can be prepared from a solution of  $[(\text{NC})_5\text{Pt-Tl}(\text{bipy})_2(\text{s})]$  (**3**) by addition of cyanide ions ( $\text{CN}/\text{Tl} = 1$ ); this results in an immediate formation of  $[(\text{NC})_5\text{Pt-Tl}(\text{bipy})(\text{CN})(\text{solv})]^-$ , which is easily detected by  $^{205}\text{Tl}$  NMR. This means that one bidentate bipy ligand is replaced by a  $\text{CN}^-$  group, while the second vacant place in the coordination

(21) The assignment of the  $^{13}\text{C}$  NMR signals of the various cyanide ligands was thoroughly discussed in a recent paper from this laboratory.<sup>3b</sup>

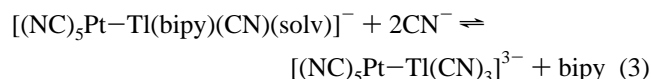
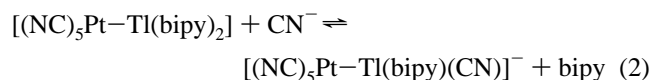
**Table 3.** Selected  $^{13}\text{C}$ ,  $^{195}\text{Pt}$ , and  $^{205}\text{Tl}$  NMR Data (Chemical Shifts (ppm) and Spin–Spin Coupling Constants (Hz)) for the Bimetallic Complexes  $[(\text{CN})_5\text{Pt}-\text{Tl}(\text{bipy})_m(\text{CN})_n(\text{solv})]^{n-}$  ( $m = 0, 1; n = 0, 1, 3$ ) and Some Related Species in Dimethyl Sulfoxide Solution<sup>a-c</sup>

	Tl	Pt	C <sup>A</sup>	C <sup>C</sup>	$^1J(\text{Tl}-\text{Pt})$	$^2J(\text{Tl}-\text{C}^A)$	$^2J(\text{Tl}-\text{C}^C)$	$^1J(\text{Pt}-\text{C}^A)$	$^1J(\text{Pt}-\text{C}^C)$
$\text{Tl}^+$	361								
$[(\text{NC})_5\text{Pt}-\text{Tl}(\text{solv})]$	887	574	84.7	83.9	65850	12213	605	920	811
$[(\text{NC})_5\text{Pt}-\text{Tl}(\text{bipy})(\text{solv})]$	1016	539	88.2	84.0	64920	11968	544	888	814
$[(\text{NC})_5\text{Pt}-\text{Tl}(\text{bipy})(\text{CN})(\text{solv})]^-$	1772	373	95.7	83.8	50130	9287	430	854	810
$[(\text{NC})_5\text{Pt}-\text{Tl}(\text{en})(\text{solv})]$	1448	494	91.3	84.7	55100	9911	480	880	816
$[(\text{NC})_5\text{Pt}-\text{Tl}(\text{en})_2(\text{solv})]$	1885	370	97.3	85.9	47850	9150	391	834	818
$[(\text{NC})_5\text{Pt}-\text{Tl}(\text{CN})_3]^{3-}$	2148				42250				
$[\text{Pt}(\text{CN})_4]^{2-}$		-189		121.6					1016

<sup>a</sup> The notation of the carbon atoms in the  $[(\text{NC})_5\text{Pt}-\text{Tl}(\text{CN})]^-$  is presented below. Solvation of the thallium atom is omitted. <sup>b</sup>  $^{205}\text{Tl}$  NMR chemical shifts are given in parts per million toward higher frequency with respect to the signal for an aqueous solution of  $\text{TlClO}_4$  extrapolated to infinite dilution at 25 °C.  $^{195}\text{Pt}$  NMR chemical shifts are given in parts per million toward higher frequency from  $X(^{195}\text{Pt}) = 21.4$  MHz and  $\delta([\text{PtCl}_6]^{2-}) = 4533$  ppm at 25 °C in aqueous solution.  $^{13}\text{C}$  NMR chemical shifts are given in parts per million relative to the solvent  $\text{DMSO}-d_6$  signal at 39.5 ppm, calibrated by the signals of TMS. <sup>c</sup> C<sup>B</sup>:  $\delta = 156$  ppm,  $^1J(\text{Tl}-\text{C}^B) = 367$  Hz.



sphere of thallium is probably filled by dmsu. A further increase of the concentration of free cyanide in the solution results in a substitution of the second bipy molecule by two  $\text{CN}^-$  ions. This is unambiguously shown by the appearance of the characteristic signal of  $[(\text{NC})_5\text{Pt}-\text{Tl}(\text{CN})_3]^{3-}$  ( $\delta_{\text{Tl}} = 2148$  ppm,  $^1J(^{205}\text{Tl}-^{195}\text{Pt}) = 42.3$  kHz) in the  $^{205}\text{Tl}$  NMR spectrum.<sup>23</sup> These considerations can be expressed by the following set of equilibrium reactions taking place in the solution:



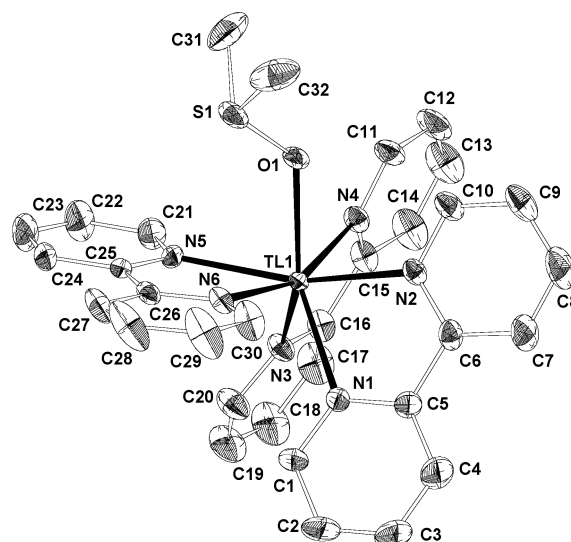
where dmsu molecule(s) can also be coordinated to the thallium. Apparently, the very high stability of monometallic<sup>9b</sup> and bimetallic<sup>22</sup> thallium cyano complexes allows the cyanide to compete with the bidentate bipy ligands for coordination to the thallium atom.

**Crystal Structures of the Tl–bipy Compounds.**  $[\text{Tl}(\text{bipy})_3(\text{dmsu})](\text{ClO}_4)_3 \cdot (\text{dmsu})_2$  (**1**). The molecular structure of the cation  $[\text{Tl}(\text{bipy})_3(\text{dmsu})]^{3+}$  is shown in Figure 4. Selected bond lengths and angles for **1** are given in Table 4. The seven-coordinated Tl atom is bonded to six nitrogen atoms of three bipy molecules and to an oxygen atom of dmsu (cf. Figure 4). The six N atoms can be viewed as confined to one hemisphere of the coordination shell and the O atom of the dmsu in the other hemisphere. The Tl1 atom is displaced 0.385(1) Å from the equatorial plane defined by N2, N4, N5, and N6. The three symmetry-

**Table 4.** Selected Bond Lengths (Å) and Angles (deg) for  $[\text{Tl}(\text{bipy})_3(\text{dmsu})](\text{ClO}_4)_3 \cdot (\text{dmsu})_2$  (**1**)

Tl1–N1	2.385(6)	Tl1–N4	2.366(6)
Tl1–N2	2.360(6)	Tl1–N5	2.378(6)
Tl1–N3	2.390(7)	Tl1–N6	2.370(6)
Tl1–O1	2.348(5)	S1–O1	1.518(6)
O1–Tl1–N1	138.3(3)	N2–Tl1–N3	123.1(2)
O1–Tl1–N2	78.7(3)	N2–Tl1–N4	85.7(2)
O1–Tl1–N3	138.5(3)	N2–Tl1–N5	159.4(3)
O1–Tl1–N4	79.0(3)	N2–Tl1–N6	99.6(2)
O1–Tl1–N5	82.7(3)	N3–Tl1–N4	69.2(2)
O1–Tl1–N6	82.5(3)	N3–Tl1–N5	77.1(3)
N1–Tl1–N2	69.4(2)	N3–Tl1–N6	121.8(2)
N1–Tl1–N3	82.7(3)	N4–Tl1–N5	99.5(2)
N1–Tl1–N4	123.0(2)	N4–Tl1–N6	159.3(3)
N1–Tl1–N5	121.7(2)	N5–Tl1–N6	68.9(3)
N1–Tl1–N6	77.3(3)		

inequivalent bite angles N1–Tl1–N2, N3–Tl1–N4, and N5–Tl1–N6 adopt approximately the same value, 69.3(3)°, 69.3(3)°, and 68.9(2)°, respectively. In two of the bipy groups

**Figure 4.** ORTEP view of the cation in  $[\text{Tl}(\text{bipy})_3(\text{dmsu})](\text{ClO}_4)_3(\text{dmsu})_2$  (compound **1**) (ellipsoids at the 20% probability level).

(22) Maliarik, M.; Glaser, J.; Tóth, I.; W. da Silva, M.; Zekany, L. *Eur. J. Inorg. Chem.* **1998**, 565.

(23)  $^{205}\text{Tl}$  NMR signals of the binuclear complexes  $[(\text{NC})_5\text{Pt}-\text{Tl}(\text{CN})_n(\text{solv})]^{n-}$  in dmsu appear at 1602, 2007, and 2148 ppm for  $n = 1, 2$ , and 3, respectively.

the pyridine rings are twisted with an angle of approximately  $11.7(6)^\circ$ , while the third bipy ligand (with N5 and N6) is more planar with a twist angle of  $2.8(6)^\circ$ . Bond lengths and angles of the bipy ligands are in accordance with those found in other complexes of the third main group cations with a 2,2'-bipyridine ligand.<sup>8,24</sup> The arrangement of the ligands around the Tl<sup>III</sup> atom is reminiscent of the one found previously in the crystal structures of  $[\text{Tl}(\text{edta})\text{X}]^{2-}$  (where X is  $\text{CN}^{25}$  or  $\text{OH}^8$ ), where the edta unit forms a six-coordinated “basket” comprising the metal ion while the ligand X is located on the top of the basket.

Hitherto, the crystal structure information on thallium(III) complexes with 2,2'-bipyridine was limited to a single compound,  $[\text{Tl}(\text{bipy})_2(\text{NO}_3)_3]$ .<sup>8</sup> In this structure, in contrast to **1**, thallium is eight-coordinated because of an additional bonding to four oxygen atoms of three nitrate groups. The higher coordination number of thallium results in somewhat longer mean Tl–N distances ( $2.392 \text{ \AA}$ ) in this compound compared to **1** ( $2.371 \text{ \AA}$ , Table 4). Two of the  $\text{NO}_3^-$  anions coordinate in a monodentate fashion, while the third is bidentate. Other examples of thallium(III) complexes with pyridine derivatives include  $[\text{Tl}(\text{CH}_3)_2(\text{phen})]\text{ClO}_4$ ,<sup>26</sup>  $[\text{TlCl}_3(\text{phen})]$ ,<sup>27</sup>  $[\text{TlCl}_2(\text{phen})_2]\text{ClO}_4$ ,<sup>6c</sup> and  $[\text{Tl}(\text{terpy})(\text{NO}_3)_3]$ ,<sup>8</sup> in which thallium is four-, five-, and seven-coordinated, respectively.

Coordination of dmsO groups to the Tl atoms is rather scarce and has hitherto been reported only for three mononuclear compounds,  $[\text{Tl}(\text{dmsO})_6](\text{ClO}_4)_3$ ,<sup>10</sup>  $[\text{TlCl}_5(\text{dmsO})](\text{Hpyr})_2$ ,<sup>28</sup>  $[\text{TlMe}_2(\text{isaTSC})(\text{dmsO})]$ ,<sup>29</sup> and for two binuclear compounds,  $[(\text{NC})_5\text{Pt}-\text{Tl}(\text{dmsO})_4]\cdot\text{dmsO}$ <sup>6b</sup> and  $[(\text{NC})_5\text{Pt}-\text{Tl}(\text{bipy})(\text{dmsO})_3]$  (this work). In  $[\text{TlCl}_5(\text{dmsO})]^{2-}$ , the presence of chloride ions and the *trans* influence result in a substantial elongation of the Tl–O bond ( $2.42 \text{ \AA}$ ) compared to that in  $[\text{Tl}(\text{dmsO})_6]^{3+}$  ( $2.224 \text{ \AA}$ ). Despite the higher coordination number of thallium in  $[\text{Tl}(\text{bipy})_3(\text{dmsO})]^{3+}$ , the present Tl1–O11 bond length of  $2.333(10) \text{ \AA}$  is significantly shorter than that in the chloride complex. In the bimetallic Pt–Tl compounds the mean Tl–O distance increases with an increasing coordination number of thallium:  $2.295 \text{ \AA}$  for five-coordinated Tl (in  $[(\text{NC})_5\text{Pt}-\text{Tl}(\text{dmsO})_4]$ ) and  $2.456 \text{ \AA}$  for six-coordinated Tl (in  $[(\text{NC})_5\text{Pt}-\text{Tl}(\text{bipy})(\text{dmsO})_3]$ ).

**$[(\text{NC})_5\text{PtTl}(\text{dmsO})_3(\text{bipy})]$  (**2**) and  **$[(\text{NC})_5\text{PtTl}(\text{bipy})_2]$  (**3**).** The molecular structures of compounds **2** and **3** are shown in Figures 5 and 6, respectively. Selected bond lengths and angles in **2** and **3** are given in Tables 5 and 6, respectively.**

The main structural feature of these bimetallic compounds is certainly the very short and unbuttressed Pt–Tl bond:

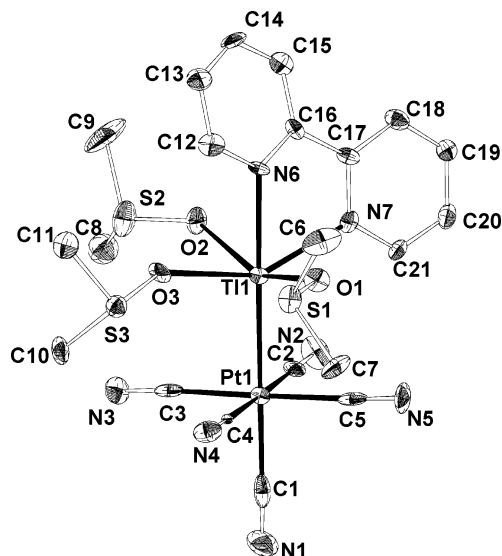


**Figure 5.** ORTEP view of the molecular structure of  $[(\text{NC})_5\text{Pt}-\text{Tl}(\text{bipy})-(\text{dmsO})_3]$  (compound **2**) (ellipsoids at the 50% probability level).

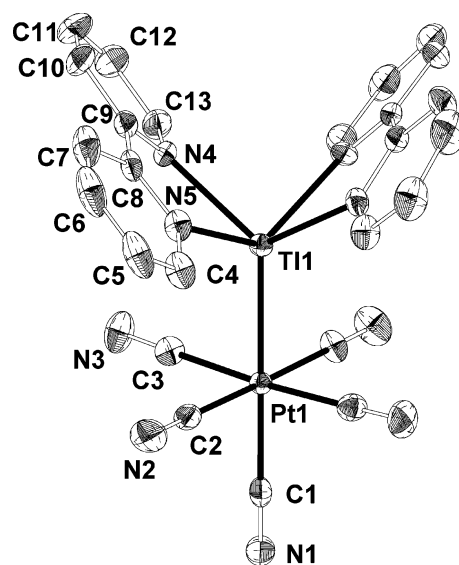


**Figure 6.** ORTEP view of the molecular structure of  $[(\text{NC})_5\text{Pt}-\text{Tl}(\text{bipy})_2]$  (compound **3**) (ellipsoids at the 30% probability level). Labels on symmetry-equivalent atoms are omitted for clarity.

$2.6187(7)$  and  $2.6117(5) \text{ \AA}$  for compounds **2** and **3**, respectively. The distances fall into the range of values obtained for the family of related compounds, all containing  $[(\text{NC})_5\text{Pt}-\text{Tl}(\text{L})_m]$  (L = ligand) entities with a variety of ligands coordinated to the thallium site:  $[(\text{NC})_5\text{Pt}-\text{Tl}(\text{CN})_n(\text{aq})]^{n-}$  ( $n = 0-3$ ; Pt–Tl =  $2.598-2.638 \text{ \AA}$ ),<sup>3c,d</sup>  $[(\text{NC})_5\text{Pt}-\text{Tl}(\text{dmsO})_4]$  (Pt–Tl =  $2.613 \text{ \AA}$ ),<sup>6b</sup>  $[(\text{NC})_5\text{Pt}-\text{Tl}(\text{en})_2]$  (Pt–Tl =  $2.635 \text{ \AA}$ ),<sup>6b</sup> and  $[(\text{NC})_5\text{Pt}-\text{Tl}(\text{phen})_m(\text{solv})]$  ( $m = 1, 2$ ; solv = dmsO; Pt–Tl =  $2.630-2.638 \text{ \AA}$ ).<sup>6c</sup> The differences in the metal–metal separations are attributed to the composition and to the geometry of the thallium coordination environment in the complexes. For the compounds where these two factors are similar, e.g.,  $[(\text{NC})_5\text{Pt}-\text{Tl}(\text{en})_2]$  and  $[(\text{NC})_5\text{Pt}-\text{Tl}(\text{bipy})_2]$ , both containing two pairs of bidentate nitrogen-donor ligands, the individual properties of the ligands are of importance. Compared to ethylenediamine, 2,2'-bipyridine is a less basic, a more rigid, and a larger

- (24) (a) Bellavance, P. L.; Corey, E. P.; Corey, J. Y.; Hey, G. W. *Inorg. Chem.* **1977**, *16*, 462. (b) Restivo, R.; Palenik, G. J. *J. Chem. Soc. D* **1972**, 341. (c) Malyarick, M. A.; Petrosyants, S. P.; Ilyuhin, A. B. *Polyhedron* **1992**, *11*, 1067. (d) Ilyuhin, A. B.; Malyarick, M. A. *Russ. J. Inorg. Chem.* **1999**, *44*, 1432.
- (25) Blixt, J.; Glaser, J.; Solymosi, P.; Tóth, I. *Inorg. Chem.* **1992**, *31*, 5288.
- (26) Blundell, T. L.; Powell, H. M. *Proc. R. Soc. London, A* **1972**, *331*, 161.
- (27) Baxter, W. J.; Gafner, G. *Inorg. Chem.* **1972**, *11*, 176.
- (28) James, B. D.; Millikan, M. B.; Mackay, M. F. *Inorg. Chim. Acta* **1983**, *77*, L251.
- (29) Casas, J. S.; Castellano, E. E.; Garcia Tasende, M. S.; Sanchez, A.; Sordo, J. *Inorg. Chim. Acta* **2000**, *304*, 283.



**Table 5.** Selected Bond Lengths (Å) and Angles (°) for [(NC)<sub>5</sub>Pt–Tl(bipy)(dmsO)<sub>3</sub>] (**2**)

Tl1–Pt1	2.6186(8)	S1–O1	1.512(9)
Tl1–O1	2.458(8)	S1–C6	1.801(15)
Tl1–O2	2.462(10)	S1–C7	1.785(16)
Tl1–O3	2.449(9)	S2–O2	1.509(9)
Tl1–N6	2.311(9)	S2–C8	1.763(16)
Tl1–N7	2.456(10)	S2–C9	1.803(18)
Pt1–C1	2.071(16)	S3–O3	1.525(10)
Pt1–C2	2.044(15)	S3–C10	1.778(13)
Pt1–C3	2.033(14)	S3–C11	1.760(13)
Pt1–C4	2.020(13)		
Pt1–C5	2.068(14)		
Pt1–Tl1–O1	101.78(18)	C3–Pt1–C5	178.0(5)
Pt1–Tl1–O2	104.7(2)	C4–Pt1–C5	88.9(5)
Pt1–Tl1–O3	100.70(17)	O1–S1–C6	104.7(6)
Pt1–Tl1–N6	177.5(3)	O1–S1–C7	105.5(6)
Pt1–Tl1–N7	107.7(2)	C6–S1–C7	98.6(7)
O1–Tl1–O2	153.4(3)	O2–S2–C8	104.2(7)
O1–Tl1–O3	87.4(3)	O2–S2–C9	104.3(7)
O1–Tl1–N6	79.9(3)	C8–S2–C9	98.3(8)
O1–Tl1–N7	91.3(3)	O3–S3–C10	105.8(6)
O2–Tl1–O3	85.5(3)	O3–S3–C11	103.7(6)
O2–Tl1–N6	73.7(3)	C10–S3–C11	99.5(6)
O2–Tl1–N7	83.0(3)	Tl1–O1–S1	126.8(5)
O3–Tl1–N6	81.2(3)	Tl1–O2–S2	123.1(6)
O3–Tl1–N7	151.2(3)	Tl1–O3–S3	147.4(5)
N6–Tl1–N7	70.3(3)	Tl1–N6–C12	119.5(8)
Tl1–Pt1–C1	179.3(4)	Tl1–N6–C16	116.8(8)
Tl1–Pt1–C2	89.8(3)	Tl1–N7–C17	114.0(8)
Tl1–Pt1–C3	91.9(4)	Tl1–N7–C21	126.8(8)
Tl1–Pt1–C4	88.3(3)	Pt1–C1–N1	179.1(13)
Tl1–Pt1–C5	86.6(4)	Pt1–C2–N2	177.4(11)
C1–Pt1–C2	90.8(5)	Pt1–C3–N3	176.7(12)
C1–Pt1–C3	88.6(5)	Pt1–C4–N4	178.8(11)
C1–Pt1–C4	91.2(5)	Pt1–C5–N5	177.1(12)
C1–Pt1–C5	92.9(5)		
C2–Pt1–C3	90.8(6)		
C2–Pt1–C4	178.0(4)		
C2–Pt1–C5	90.5(6)		
C3–Pt1–C4	89.8(5)		

**Table 6.** Selected Bond Lengths (Å) and Angles (°) for [(NC)<sub>5</sub>Pt–Tl(bipy)<sub>2</sub>] (**3**)<sup>a</sup>

Tl1–Pt1	2.6117(5)	C4–C5	1.366(11)
Tl1–N4	2.358(5)	C5–C6	1.370(12)
Tl1–N5	2.403(5)	C6–C7	1.373(13)
Pt1–C1	2.061(9)	C7–C8	1.404(10)
Pt1–C2	2.025(7)	C8–C9	1.488(9)
Pt1–C3	2.021(7)	C9–C10	1.385(10)
N1–C1	1.112(11)	C10–C11	1.362(15)
N2–C2	1.106(9)	C11–C12	1.366(13)
N3–C3	1.114(10)	C12–C13	1.376(11)
N4–C9	1.339(8)		
N4–C13	1.339(8)		
N5–C4	1.347(8)		
N5–C8	1.326(8)		
Pt1–Tl1–N4	122.74(12)	C1–Pt1–C3	92.06(14)
Pt1–Tl1–N5	115.96(12)	C2–Pt1–C3	89.2(3)
N4–Tl1–N5	68.78(17)	C2–Pt1–C2 <sup>i</sup>	178.6(2)
N4–Tl1–N4 <sup>i</sup>	114.51(17)	C2–Pt1–C3 <sup>i</sup>	90.7(3)
N4–Tl1–N5 <sup>i</sup>	83.59(17)	C3–Pt1–C3 <sup>i</sup>	175.88(19)
N5–Tl1–N5 <sup>i</sup>	128.07(16)	Tl1–N5–C4	122.6(4)
N4 <sup>i</sup> –Tl1–N5 <sup>i</sup>	68.78(17)	Tl1–N5–C8	117.0(4)
Tl1–Pt1–C1	180.0(4)	C4–N5–C8	120.3(5)
Tl1–Pt1–C2	89.29(14)	Pt1–C1–N1	180.0(14)
Tl1–Pt1–C3	87.94(14)	Pt1–C2–N2	179.1(6)
C1–Pt1–C2	90.71(14)	Pt1–C3–N3	178.6(5)

<sup>a</sup> i indicates 1/2 – x, y, –z.

ligand.<sup>30</sup> The lower basicity results in a weaker thallium–bipy interaction in [(NC)<sub>5</sub>Pt–Tl(bipy)<sub>2</sub>], which in turn leads to stronger metal–metal bonding.

In addition to the Pt–Tl linkage, the platinum atom in both compounds is bonded to five carbons of the cyanide ligands; in **3** the CN groups are symmetry-related to each other. Four *cis* carbon atoms constitute an almost square plane around the platinum atom, while the fifth carbon occupies an axial position in the pseudooctahedron, *trans* to the thallium atom. The *cis* Pt–C distances in **2** vary, and one of the values is not significantly different from that for the *trans* Pt–C bond (Table 5). In contrast, in structure **3** with a higher molecular symmetry (*C*<sub>2v</sub>), the difference in platinum–carbon separations between the two geometrical positions of the carbon atoms is distinct. The *trans* Pt–C1 bond is longer (by ca. 0.04 Å) than the two *cis* bonds, Pt–C2 and Pt–C3 (Table 6). A similar, and even more pronounced, *trans* lengthening effect was observed in the structure of a symmetry-related compound, [(NC)<sub>5</sub>Pt–Tl(en)<sub>2</sub>], with an axial Pt–C distance exceeding the equatorial ones by more than 0.07 Å.<sup>6b</sup> This is assumed to be due to the *trans* influence of the X ligand in the pseudooctahedral complex [(NC)<sub>5</sub>Pt–X]; this effect is well-known for a large number of  $\sigma$ -bonded complexes of transition metals.<sup>31</sup>

Apart from the metal–metal bond, the Tl atom is also linked to either two (one bipy molecule) or four (two bipy molecules) N atoms in the structures of **2** and **3**, respectively. In structure **2**, apart from one bipy ligand, thallium also coordinates three dmsO molecules, leading to a distorted octahedral geometry of the coordination polyhedron (Figure 5). Atoms O1, O2, O3, and N7 define an equatorial plane within 0.02 Å. The Tl atom is displaced 0.582(1) Å from this plane toward the Pt atom. The second nitrogen atom of the bipy ligand, N6, occupies an axial position in the thallium pseudooctahedron, *trans* to the platinum atom. The two pyridine rings in the bipy group are also twisted toward each other with an angle of 15.4(6)°. The different locations of the two nitrogen atoms, in terms of the atoms occupying *trans* positions to them in the thallium coordination sphere (O3 for N7, and Pt for N6), result in an essential difference in the bond lengths: 2.311 and 2.456 Å for Tl–N6 and Tl–N7, respectively.

In structure **3** with two bipy ligands, thallium is five-coordinated and the ligands form a distorted square pyramid (Figure 6). The pyramidal base consisting of nitrogen atoms N4, N4', N5, and N5' adopts a rectangular shape (the largest deviation of the atoms from the mean plane is 0.11 Å). The Tl atom in the apical position is 1.164(1) Å above this plane. The variation of the Tl–N bond lengths is much less pronounced, 2.358 and 2.403 Å, than in structure **2**.

Another notable feature of the molecular geometry of the two complexes is the mutual arrangement between the Pt–(CN)<sub>4</sub> and Tl(O<sub>3</sub>N) and Tl(N<sub>4</sub>) units. The four equatorial ligand atoms around Tl are in a staggered conformation to the adjacent square planar Pt(CN)<sub>4</sub> unit in structure **2**, while

(30) House, D. A. In *Encyclopedia of Inorganic Chemistry*; King, R. B., Ed.; John Wiley and Sons: Chichester, U.K., 1995; Vol. 1.

(31) Levin, A. A.; Dyachkov, P. N. *Electronic structure, geometry, isomerism and transformations in heteroligand molecules*; Nauka: Moscow, 1990.

in **3**, an eclipsed conformation between the two bipy groups and the *cis*-cyanide ions is favored.

**Metal–Metal Bonding in [(NC)<sub>5</sub>Pt–Tl(bipy)<sub>m</sub>(CN)<sub>n</sub>–(solvent)]<sup>n–</sup> Complexes (*m* = 0, 1; *n* = 0, 1).** The characteristic frequencies attributed to Pt–Tl stretching vibrations for the complexes [(NC)<sub>5</sub>Pt–Tl(CN)<sub>n</sub>(aq)]<sup>n–</sup> (*n* = 0–3) in aqueous solution appear as strong and sharp Raman bands at 157–161 cm<sup>–1</sup>,<sup>3b</sup> for the solid compound (NC)<sub>5</sub>PtTl four bands belonging to the metal–metal stretch are found in the range between 152 and 211 cm<sup>–1</sup>.<sup>3d</sup> The corresponding bands for the crystalline compounds [(NC)<sub>5</sub>Pt–Tl(dmsol)<sub>3</sub>(bipy)] and [(NC)<sub>5</sub>Pt–Tl(bipy)<sub>2</sub>] are detected at 153 and 169 cm<sup>–1</sup>, respectively. The Pt–Tl force constants in the molecules, 1.38 and 1.68 N/cm, respectively, have been estimated using the diatomic oscillator approximation.<sup>32</sup> This is close to the values calculated for the parent Pt–Tl cyanide complexes (1.45–1.53 N/cm)<sup>3c</sup> and is still attributed to a single metal–metal bond.<sup>33</sup> The Pt–Tl force constants for complexes **2** and **3** in solution are compatible with the corresponding Pt–Tl bond distances in the solid state, 2.6187(7) and 2.6117–(5) Å, respectively.

Similarly to the previously studied family of complexes [(NC)<sub>5</sub>Pt–Tl(CN)<sub>n</sub>(aq)]<sup>n–</sup> (*n* = 0–3) in an aqueous medium,<sup>3b</sup> and [(NC)<sub>5</sub>Pt–Tl(solvent)] and [(NC)<sub>5</sub>Pt–Tl(en)<sub>m</sub>(solvent)] (*m* = 1, 2) species in dimethyl sulfoxide solution,<sup>6b</sup> the bimetallic Pt–Tl–bipy compounds in dmsol exhibit very large values of one-bond <sup>195</sup>Pt–<sup>205</sup>Tl spin–spin coupling constants (Table 3). This strong coupling is a characteristic feature of the bonding between the two metals with the formal oxidation states {Pt<sup>II</sup>–Tl<sup>III</sup>}, and is an indication of a significant contribution of thallium 6s orbitals to the metal–metal bonding.<sup>3b</sup> Among several known compounds with closed-shell metal–metal interactions between the same metal atoms, namely, {Pt<sup>0</sup>–Tl<sup>I</sup>} and {Pt<sup>II</sup>–Tl<sup>I</sup>} systems with d<sup>10</sup>–s<sup>2</sup> and d<sup>8</sup>–s<sup>2</sup> electron configurations, respectively,<sup>34,35</sup> only a few can exist in solution. Pt–Tl bonds readily dissociate when the compounds are dissolved in polar coordinating solvents, which indicates a weakness of the metal–metal bonding. In the few cases where the coupling constant <sup>1</sup>J(<sup>195</sup>Pt–<sup>205</sup>Tl)

for molecules with {Pt<sup>0</sup>–Tl<sup>I</sup>} and {Pt<sup>II</sup>–Tl<sup>I</sup>} bonds could be measured,<sup>1a,34a,c,35b</sup> its values are at least 1 order of magnitude lower than those in {Pt<sup>II</sup>–Tl<sup>III</sup>} compounds. Such a pronounced drop of the <sup>1</sup>J(<sup>195</sup>Pt–<sup>205</sup>Tl) values is consistent with a minor participation of the thallium 6s electrons in the spin–spin coupling. This should be attributed to the 6s<sup>2</sup> “inert pair” effect, which is a classical feature for thallium chemistry.<sup>12</sup>

Apart from the very large values of <sup>1</sup>J(<sup>195</sup>Pt–<sup>205</sup>Tl) in the family of binuclear compounds, there is also a remarkably strong two-bond spin–spin coupling <sup>205</sup>Tl–<sup>13</sup>C for the cyano ligand occupying a *trans* position (CN<sup>A</sup>) to the thallium atom in the pseudooctahedral platinum coordination (see Table 2). The values of <sup>2</sup>J(<sup>205</sup>Tl–<sup>13</sup>C<sup>A</sup>) are more than 20 times larger than the coupling constants between thallium and four equivalent cyano groups in *cis* positions, <sup>2</sup>J(<sup>205</sup>Tl–<sup>13</sup>C<sup>C</sup>). Moreover, in ref 3b we observed that <sup>2</sup>J(<sup>205</sup>Tl–<sup>13</sup>C<sup>A</sup>) ≫ <sup>1</sup>J(<sup>205</sup>Tl–<sup>13</sup>C<sup>B</sup>). This indicates a very intense orbital overlap in the linear C<sup>A</sup>–Pt–Tl pattern.<sup>3b</sup> A theoretical investigation of this spin–spin coupling pattern reveals remarkable electron delocalization within multicenter C<sup>A</sup>–Pt–Tl bonding which seems to be responsible for the large magnitude of <sup>2</sup>J(<sup>205</sup>Tl–<sup>13</sup>C<sup>A</sup>) in the complexes.<sup>4a</sup>

Although the values of <sup>1</sup>J(<sup>195</sup>Pt–<sup>205</sup>Tl) are strongly dependent on the variations of the s character in the Pt–Tl bond, it was recently found that there is usually a good correlation between the spin–spin coupling and both the metal–metal separation and the bond strength. An EXAFS study of the series of [(NC)<sub>5</sub>Pt–Tl(CN)<sub>n</sub>(aq)]<sup>n–</sup> complexes in aqueous solution revealed an expected increase of the Pt–Tl distance with the decrease of <sup>1</sup>J(<sup>195</sup>Pt–<sup>205</sup>Tl) for the corresponding complexes.<sup>3c</sup>

In the same way as for the species [(NC)<sub>5</sub>Pt–Tl(CN)<sub>n</sub>–(aq)]<sup>n–</sup> in aqueous solution, coordination of additional ligands to the thallium site of the molecules results in a decrease of the coupling constant. Thus, when a bipy molecule is coordinated to the thallium atom in the [(NC)<sub>5</sub>Pt–Tl(solvent)] complex in dimethyl sulfoxide, <sup>1</sup>J(<sup>195</sup>Pt–<sup>205</sup>Tl) decreases by ~1000 Hz (Table 3).<sup>36</sup> This reduction of the coupling constant is reflected by a slight lengthening of the metal–metal bond: Pt–Tl = 2.6131(4) Å in [(NC)<sub>5</sub>Pt–Tl(dmsol)<sub>4</sub>] and 2.6187(7) Å in [(NC)<sub>5</sub>Pt–Tl(bipy)(dmsol)<sub>3</sub>]. A more dramatic drop of the constant (almost 15000 Hz) occurs when a cyanide ion is added to the thallium coordination sphere, yielding the complex [(NC)<sub>5</sub>Pt–Tl(bipy)(CN)(solvent)]<sup>–</sup>; this effect is typical for the coordination of CN<sup>–</sup> ions to the Pt–Tl bond.<sup>3b</sup> Consequently, a pronounced increase of the metal–metal separation in the latter compound can be anticipated.

In an overview of the platinum–thallium bond distances for the hitherto structurally characterized compounds, four groups can be distinguished depending on the formal oxidation states of the metal ions: Pt<sup>0</sup>–Tl<sup>I</sup> (2.860–3.127 Å),<sup>1,34</sup> Pt<sup>II</sup>–Tl<sup>I</sup> (2.796–3.152 Å),<sup>35</sup> Pt<sup>II</sup>–Tl<sup>II</sup> (2.698–2.708 Å),<sup>37</sup> and Pt<sup>II</sup>–Tl<sup>III</sup> (2.598–2.638 Å).<sup>3c,d,6b,c</sup> Considering only

- (32) (a) The force constant (N/cm) was calculated from  $k = (5.889 \times 10^{-7})\nu^2\mu$ , where  $\nu$  is the frequency (cm<sup>–1</sup>) and  $\mu = M_{\text{Pt}}M_{\text{Tl}}/(M_{\text{Pt}} + M_{\text{Tl}})$  with atomic masses of the metals in daltons. (b) A recently completed calculation of the metal–metal stretching force constants in complexes [(NC)<sub>5</sub>Pt–Tl(CN)<sub>n</sub>]<sup>n–</sup> shows that, in a full model, taking into account all (both metal–metal and metal–ligand) vibrational modes, about 92% is attributed to the purely diatomic Pt–Tl stretch.<sup>3b,c</sup>  
 (33) Cotton, F. A.; Walton, R. A. *Multiple Bonds Between Metal Atoms*, 2nd ed.; Clarendon Press: Oxford, 1993.  
 (34) (a) Ezomo, O. J.; Mingos, M. P.; Williams, I. D. *J. Chem. Soc., Chem. Commun.* **1987**, 924. (b) Hao, L.; Vittal, J. J.; Puddephatt, R. J. *Inorg. Chem.* **1996**, *35*, 269. (c) Catalano, V. J.; Bennett, B. L.; Yson, R. L.; Noll, B. C. *J. Am. Chem. Soc.* **2000**, *122*, 10056. (d) Stadnichenko, R.; Sterenberg, B. T.; Bradford, A. M.; Jennings, M. C.; Puddephatt, R. J. *J. Chem. Soc., Dalton Trans.* **2002**, 1212. (e) Mednikov, E. G.; Dahl, L. F. *Dalton Trans.* **2003**, 3117.  
 (35) (a) Nagle, J. K.; Balch, A. L.; Olmstead, M. M. *J. Am. Chem. Soc.* **1988**, *110*, 319. (b) Balch, A. L.; Rowley, S. P. *J. Am. Chem. Soc.* **1990**, *112*, 6139. (c) Renn, O.; Lippert, B. *Inorg. Chim. Acta* **1993**, *208*, 219. (d) Klepp, K. O. *J. Alloys Compd.* **1993**, *196*, 25. (e) Bronger, W.; Bonsmann, B. Z. *Anorg. Allg. Chem.* **1995**, *621*, 2083. (f) Uson, R.; Fornies, J.; Tomas, M.; Garde, R.; Merino, R. I. *Inorg. Chem.* **1997**, *36*, 1383. (g) Ara, I.; Berenguer, J. R.; Fornies, J.; Gomez, J.; Lalinde, E.; Merino, R. I. *Inorg. Chem.* **1997**, *36*, 6461. (h) Song, H.-B.; Zhang, Z.-Z.; Hui, Z.; Che, C.-M.; Mak, T. C. W. *Inorg. Chem.* **2002**, *41*, 3146.

- (36) This description is oversimplified, since the solvation of the thallium atom is not taken into account; however, in the cases of both water and dmsol, the impact of the solvent on the nuclear spin–spin coupling (and bonding) is much smaller compared to the ligand coordination.

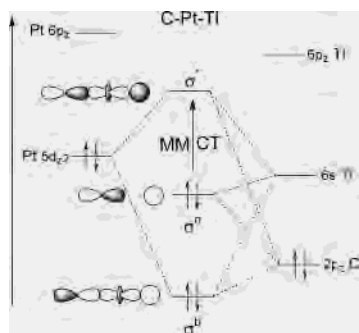


**Figure 7.** A qualitative molecular orbital diagram illustrating  $\sigma$ -bonding within the NC–Pt–Tl fragment of the  $\{(\text{NC})_5\text{Pt-Tl}\}$  unit ( $C_{4v}$  symmetry) appearing as a stable building block in all complexes  $[(\text{NC})_5\text{Pt-Tl}(\text{L})_m]$  (L = ligand). The values of the orbital energies for Pt( $d_{z^2}$ ), 8.8 eV, and for Tl( $6s$ ), 10.2 eV, were taken from refs 41 and 42.

the compounds of bivalent platinum, it appears that the Pt–Tl bond becomes shorter when the formal oxidation state of thallium increases from Tl<sup>I</sup> to Tl<sup>III</sup>. This is consistent with both the decreasing size of the thallium cation and strengthening of the metal–metal interaction due to stronger contribution of the thallium 6s orbitals in the bonding.

Very recently, Pyykkö and Patzschke have carried out a computational study of model compounds  $[\text{H}_5\text{Pt-TlH}_m]^{n-}$  serving as analogues to the  $[(\text{NC})_5\text{Pt-Tl}(\text{CN})]^{n-}$  species.<sup>38</sup> The authors suggest that the short metal–metal bonds for the experimentally known complexes and their hydride models can be explained by some triple bond character of the Pt–Tl interaction. The bonding is argued to be composed of two opposite donor–acceptor processes:  $\sigma$ , which is a thallium 6s lone pair  $\rightarrow$  Pt donation, and Pt  $\rightarrow$  Tl( $6p$ )  $\pi$  donation. While  $\sigma$  orbital interaction is dominating, the  $\pi$  part is not found to be negligible. Although such a multiple bond model can account for relatively short Pt–Tl separations in the complexes, we do not think it is chemically relevant. As we already noted above, the experimental data are not compatible with the presence of a lone electron pair at the thallium 6s orbital. Furthermore, considering the Pt–Tl bonded molecules to be built of Pt<sup>IV</sup> and Tl<sup>I</sup> fragments seems to be an artificial approach since the formation reaction occurs between the Pt<sup>II</sup> and Tl<sup>III</sup> species. Pt<sup>IV</sup> and Tl<sup>I</sup>, on the other hand, represent oxidation states of the reaction products of a nonreversible two-electron transfer occurring in the family of the Pt–Tl cyano complexes and can hardly yield metal–metal bonding.<sup>5a</sup>

In a qualitative description, it should be rather Pt( $5d_{z^2}$ )  $\rightarrow$  Tl( $6s$ ) donation which gives rise to  $\sigma$  bonding. However, this is an oversimplified picture of the bond, which does not take into account a significant electron delocalization within the linear  $\text{C}^{\text{A}}\text{-Pt-Tl}$  pattern.<sup>3b,4a</sup> The latter phenomenon can be best illustrated by a qualitative molecular orbital diagram (Figure 7) constructed for a pseudooctahedral  $\{(\text{NC})_5\text{Pt-Tl}\}$  unit. This unit is a stable building block in the family of Pt<sup>II</sup>–Tl<sup>III</sup> cyano species (vide supra), where thallium can be treated as a ligand coordinated to the platinum atom.

Considering only the valence orbitals giving rise to  $\sigma$  bonding, thallium 6s and carbon 2p<sub>z</sub> match in symmetry ( $A_1$  in the  $C_{4v}$  geometry) with platinum 5d<sub>z<sup>2</sup></sub> (HOMO for  $[\text{Pt}(\text{CN})_4]^{2-}$ ) and can form a set of molecular orbitals.<sup>39</sup>

The optical properties of the binuclear complexes  $[(\text{NC})_5\text{Pt-Tl}(\text{CN})_n(\text{aq})]^{n-}$  ( $n = 0-3$ ) in aqueous solution are dominated by the metal–metal interaction. Upon mixing solutions of  $[\text{Pt}(\text{CN})_4]^{2-}$  and  $[\text{Tl}(\text{CN})_n(\text{aq})]^{3-n}$ , a new and very intensive electronic absorption band appears in the UV region of the spectra, in the range 238–259 nm ( $\epsilon = 2.9-6.9 \times 10^4 \text{ M}^{-1} \text{ cm}^{-1}$ ), depending on the concentration of cyanide (Figure 8a). In all cases the band is almost perfectly described by a single Gaussian contour. The appearance of the band is attributed to the formation of the bimetallic species since thallium cyano complexes have negligible absorption in this region while one of the strongest bands of tetracyanoplatinate, at 253 nm, has significantly lower extinction. The band is very sensitive to the change of solvent, and a pronounced red shift of the absorption occurs when the solvent is changed from water to dimethyl sulfoxide (294 nm,  $\epsilon = 2.1 \times 10^4 \text{ M}^{-1} \text{ cm}^{-1}$ ; cf. Figure 8b). The very large extinction coefficient of the band and its solvatochromic behavior point to the charge-transfer nature of the electronic transition.<sup>40a</sup> Due to the fact that the complexes exhibit a polar metal–metal bond between two different metal ions in their reducing and oxidizing forms, respectively, the absorption is assigned to the metal-to-metal charge-transfer (MMCT) transition (Figure 7).<sup>40b,c</sup>

The effect of coordinated bipy molecules on the electronic absorption spectra of the bimetallic complexes is shown in Figure 8c (for comparison, the spectrum of the related species  $[\text{Tl}(\text{bipy})_m(\text{sol})]^{3+}$  in dimethyl sulfoxide solution is also displayed). Because of the equilibria between the  $[(\text{NC})_5\text{Pt-Tl}(\text{bipy})_m(\text{sol})]$  species in solution, and the narrow energy range of their corresponding electronic transitions, no individual bands of the complexes can be distinguished (similar problems hamper detection of individual bands of  $[\text{Tl}(\text{bipy})_m(\text{sol})]^{3+}$  species). Compared to that of  $[(\text{NC})_5\text{Pt-Tl}(\text{sol})]$ , the spectra of the species  $[(\text{NC})_5\text{Pt-Tl}(\text{bipy})_m(\text{sol})]$  have a more complex band shape. This can be related to the electronic transitions occurring between the orbitals largely confined to the bipy ligand and the Tl–bipy entity of the complex. Especially intense are intraligand ( $\pi \rightarrow \pi^*$ ) transitions. Thus, the strongest band of 2,2'-bipyridine in

(37) Uson, R.; Fornies, J.; Tomas, M.; Garde, R.; Alonso, P. *J. Am. Chem. Soc.* **1995**, *117*, 1837.

(38) Pyykkö, P.; Ratzschke, M. *Faraday Discuss.* **2003**, *124*, 41.

(39) CN<sup>-</sup>: the HOMO of the cyano group is a  $\sigma$  orbital, to which the electron pair localized on the carbon 2p<sub>z</sub> atomic orbital can be largely assigned. Golub, A. M.; Köller, H.; Skopenko, V. V. *Chemistry of Pseudohalides*; Elsevier: Amsterdam, 1986.  $[\text{Pt}(\text{CN})_4]^{2-}$ : Ziegler, T.; Nagle, J.; Snijders, J. G.; Baerends, E. J. *J. Am. Chem. Soc.* **1989**, *111*, 5631.

(40) (a) Horvath, O.; Stevenson, K. L. *Charge Transfer Photochemistry of Coordination Compounds*; VCH Publishers: New York, 1993; (b) Lever, A. B. P. *Inorganic Electronic Spectroscopy*; Elsevier: Amsterdam, 1984. (c) Vogler, A.; Kunkely, H. In *Photosensitization and Photocatalysis Using Inorganic and Organometallic Compounds*; Kalyanasundaram, K., Grätzel, M., Eds.; Kluwer Academic Publishers: Dordrecht, The Netherlands, 1993; Vol. 14, pp 88–107.

(41) Louwen, J. N.; Hengelmolen, R.; Grove, D. M.; Oskam, A. *Organometallics* **1984**, *3*, 908.

(42) Schweitzer, G. K.; McMurtrie, A. C.; Allen, J. D.; Cusachs, L. C.; Vick, D. O.; Finkelstein, G. *J. Electron Spectrosc. Relat. Phenom.* **1977**, *10*, 155.

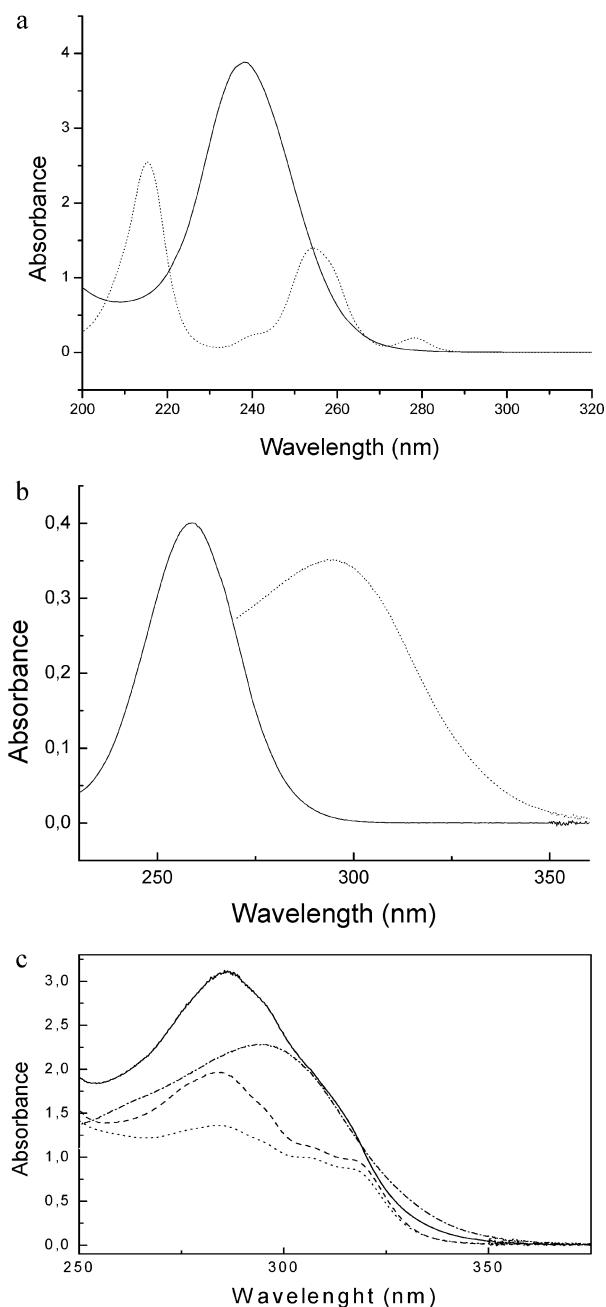


**Figure 8.** Electronic absorption spectra of solid compounds dissolved in (a) water,  $8.6 \times 10^{-4}$  M  $[(\text{NC})_5\text{Pt}-\text{Tl}(\text{CN})]^-$  (solid line) and  $1.20 \times 10^{-3}$  M  $[\text{Pt}(\text{CN})_4]^{2-}$  (dashed line), (b) water,  $9.4 \times 10^{-4}$  M  $[(\text{NC})_5\text{Pt}-\text{Tl}]$  (solid line), and dimethyl sulfoxide,  $1.12 \times 10^{-3}$  M  $[(\text{NC})_5\text{Pt}-\text{Tl}]$  (dashed line), and (c) dimethyl sulfoxide,  $8.3 \times 10^{-4}$  M  $[(\text{NC})_5\text{Pt}-\text{Tl}(\text{bipy})_2]$  (solid line),  $1.12 \times 10^{-3}$  M  $[(\text{NC})_5\text{Pt}-\text{Tl}]$  (dashed-dotted line),  $1.18 \times 10^{-3}$  M  $[\text{Tl}(\text{dmsO})_6]^{3+} + 1.18 \times 10^{-3}$  M bipy (dotted line), and  $8.5 \times 10^{-4}$  M  $[\text{Tl}(\text{dmsO})_6]^{3+} + 1.70 \times 10^{-3}$  M bipy (dashed line).

dmsO appears at 284 nm with an extinction coefficient  $1.2 \times 10^4 \text{ M}^{-1} \text{ cm}^{-1}$ . The bands of the transitions attributed to the Tl–bipy entity are substantially weaker (cf. the spectra of  $[\text{Tl}(\text{bipy})_m(\text{solv})]^{3+}$  complexes (Figure 8)).

Curve fitting of the spectrum profiles for the solutions containing the complex  $[(\text{NC})_5\text{Pt}-\text{Tl}(\text{solv})]$  with some amount of added bipy can be described by at least three overlapping bands (not counting the solvent contribution at  $\leq 260$  nm). The strongest band in each set ( $\epsilon \approx 1.6 \times 10^4 \text{ M}^{-1} \text{ cm}^{-1}$  in all cases) is only slightly affected by changes

in the thallium coordination and is found to shift from 295 to 303 nm when the bipy/Tl ratio varies between 0.6 and 2.0, respectively. Both the similar energy and the intensity of the absorption band allow the assignment of this feature to the MMCT transition. It can be concluded that attachment of the bipy ligand neither shifts nor notably extends the absorption of the bimetallic complexes to the visible region. Coordination of 2,2'-bipyridine to the thallium atom in the heterobimetallic complexes has a barely significant influence on the MMCT transition compared to the solvatochromic effect, namely, a shift of the MMCT band for the complex  $[(\text{NC})_5\text{Pt}-\text{Tl}(\text{solv})]$  from 259 to 295 nm when the solvent is changed from water to dmsO, respectively.

## Conclusions

For the first time, the speciation and structure of the  $\text{Tl}^{\text{III}}$ -bipy complexes in solution was studied by means of multinuclear ( $^1\text{H}$ ,  $^{13}\text{C}$ , and  $^{205}\text{Tl}$ ) NMR spectroscopy. In both the dimethyl sulfoxide and acetonitrile solutions the signals of individual  $[\text{Tl}(\text{bipy})_m(\text{solv})]^{3+}$  ( $m = 1-3$ ) species have been observed; however, a number of solvent and ligand exchange reactions in the system prevent the detection of separate signals in some cases. The complexes are in equilibrium governed by the concentration of the ligand. No information on the tris(bipy) species could be obtained in the dmsO solution because of exchange processes; however, the crystal structure of  $[\text{Tl}(\text{bipy})_3(\text{dmsO})](\text{ClO}_4)_3(\text{dmsO})_2$  (**1**), with a seven-coordinated thallium cation, indicates that a direct coordination of dmsO to the metal can be present also in solution.

To be able to modify the properties of the bimetallic complexes  $[(\text{NC})_5\text{Pt}-\text{Tl}(\text{CN})_n(\text{solv})]^{n-}$  ( $n = 0-3$ ), their interaction with 2,2'-bipyridine in dimethyl sulfoxide solution was studied. The reaction between  $[(\text{NC})_5\text{Pt}-\text{Tl}(\text{dmsO})_4](\text{s})$  and bipy in dmsO results in the formation of  $[(\text{NC})_5\text{Pt}-\text{Tl}(\text{bipy})(\text{solv})]$ . NMR results confirm that the platinum pentacyano unit is preserved in the complex, while the bipy ligand is coordinated to the thallium "site" in the molecule. A very large one-bond  $^{195}\text{Pt}-^{205}\text{Tl}$  spin–spin coupling constant, 64.9 kHz, detected in both  $^{195}\text{Pt}$  and  $^{205}\text{Tl}$  NMR spectra of the solution, unambiguously indicates the presence of a direct metal–metal bond in the complex. The complex can alternatively be prepared by the reaction of  $[\text{Tl}(\text{bipy})(\text{solv})]^{3+}$  with  $[\text{Pt}(\text{CN})_4]^{2-}$  ion in the presence of an equimolar amount of free cyanide.

When cyanide ions are introduced to a solution of  $[(\text{NC})_5\text{Pt}-\text{Tl}(\text{bipy})(\text{solv})]$  ( $\text{CN}^-/\text{Tl} \leq 1$ ), the complex  $[(\text{NC})_5\text{Pt}-\text{Tl}(\text{bipy})(\text{CN})(\text{solv})]^-$  is formed. Coordination of the cyanide ion to the thallium substantially weakens the  $^{195}\text{Pt}-^{205}\text{Tl}$  spin–spin coupling in the compound. A further increase of the free cyanide concentration results in a substitution of bipy in the coordination sphere of thallium, and the equilibrium shifts to the homoligand species  $[(\text{NC})_5\text{Pt}-\text{Tl}(\text{CN})_3]^{3-}$ . It can therefore be concluded that despite the bidentate coordination mode and the formation of the stable five-membered chelate ring, 2,2'-bipyridine is a weaker ligand compared to cyanide, in the bimetallic Pt–Tl complexes in dmsO solution.

Two solid compounds,  $[(\text{NC})_5\text{Pt}-\text{Tl}(\text{bipy})(\text{dmsO})_3]$  (**2**) and  $[(\text{NC})_5\text{Pt}-\text{Tl}(\text{bipy})_2]$  (**3**), were crystallized from the  $(\text{NC})_5\text{Pt}-\text{Tl}-\text{bipy}-\text{dmsO}$  system. The X-ray crystal structure determination of the compounds revealed the presence of an unsupported metal–metal bond in both cases. The Pt–Tl distances of 2.6187(7) and 2.6117(5) Å for **2** and **3**, respectively, are among the shortest reported separations between these two metals. The platinum coordination is the same in both compounds—pseudooctahedral, built up by five cyano carbons and by the thallium atom. The coordination sphere of thallium is a distorted octahedron and a square pyramid for **2** and **3**, respectively. It is possible that the lower coordination number of the thallium atom in the latter case contributes to the somewhat shorter metal–metal separation. The Pt–Tl force constants in **2** and **3**, 1.38 and 1.68 N/cm, respectively, calculated using Raman frequencies of the metal–metal stretching vibrations, are compatible with the intermetallic separations and indicate a stronger bond in the bis(bipy) compound; the values of the constants are characteristic for a single metal–metal bond.

Attachment of a chromophore bipy molecule to the thallium part of the bimetallic platinum–thallium cyano compounds results in the appearance of the electronic

absorption spectra characteristic for mononuclear  $\text{Tl}^{\text{III}}-\text{bipy}$  species. An absorption band, representative for the Pt–Tl metal-to-metal charge transfer, could be discerned, but its position is almost unaffected by the coordination of 2,2'-bipyridine.

**Acknowledgment.** The continuous financial support of the Swedish Natural Science Research Council (NFR) is gratefully acknowledged. We thank the European Commission's INTAS program and the Carl Trygger Foundation for financial support and the Swedish Institute for the fellowship for G.M.'s stay in Stockholm.

**Supporting Information Available:** Figure S1 ( $^{13}\text{C}$  and  $^1\text{H}$  NMR spectra of a solution containing  $\text{Tl}^{\text{III}}$  and bipy in  $\text{DMSO}-d_6$ , and the assignments of the peaks), Figure S2 ( $^{13}\text{C}$  spectrum of  $[\text{Tl}(\text{bipy})_3(\text{dmsO})](\text{ClO}_4)_3(\text{dmsO})_2$  in  $\text{CD}_3\text{CN}$ ), and Figure S3 ( $^{205}\text{Tl}$  NMR spectra of the complex  $[(\text{NC})_4(\text{N}^{13}\text{C})\text{Pt}-\text{Tl}(\text{bipy})(\text{solv})](^{13}\text{C}-\text{CN})$  in dmsO) (PDF) and crystallographic information file (CIF) for the single-crystal structure determinations of compounds **1–3**. This material is available free of charge via the Internet at <http://pubs.acs.org>.

IC034571E